# Microbiota effects and predictors of *Lactobacillus crispatus* colonization after treatment with a vaginal live biotherapeutic: results from a randomized, double-blinded, placebo-controlled trial

**Authors & affiliations**

Seth M. Bloom*[1,2,3], Laura Symul*[4], Joseph Elsherbini[1], Jiawu Xu[1], Salina Hussain[1], Johnathan Shih[1], Ashley Sango[1], Caroline M. Mitchell[1,3,5,6], Anke Hemmerling[7], Thomas P. Parks[8], Aditi Kannan[1], Fatima A. Hussain[1,3], Craig R. Cohen[7], Susan P. Holmes[9], Douglas S. Kwon[1,2,3]

1. Ragon Institute of Mass General Brigham, MIT, and Harvard, Cambridge, Massachusetts, USA
2. Division of Infectious Diseases, Massachusetts General Hospital, Boston, Massachusetts, USA
3. Harvard Medical School, Boston, Massachusetts, USA
4. Institute of Statistics, Biostatistics and Actuarial Sciences (ISBA), Louvain Institute of Data Analysis and Modelling (LIDAM), UCLouvain, Belgium
5. Department of Obstetrics & Gynecology, Massachusetts General Hospital, Boston, Massachusetts, USA
6. Vincent Center for Reproductive Biology, Massachusetts General Hospital, Boston, Massachusetts, USA
7. Department of Obstetrics, Gynecology, & Reproductive Sciences, University of California San Francisco, San Francisco, California, USA
8. Osel, Inc., Mountain View, California, USA
9. Department of Statistics, Stanford University, Palo Alto, California, USA

*Contributed equally

Correspondence: Douglas S. Kwon, dkwon@mgh.harvard.edu

**Abstract**

Bacterial vaginosis (BV) affects >25% of women worldwide and often recurs following treatment with the standard-of-care antibiotic metronidazole (MTZ). Treatment with LACTIN-V, a live biotherapeutic product (LBP) containing the *Lactobacillus crispatus* strain CTV-05, reduced recurrent BV (rBV) in a Phase 2b clinical trial, but efficacy was incomplete. We analyzed trial samples to characterize microbiota and immune effects and identify correlates of treatment success. By week 12, an *L. crispatus*-dominant microbiota was achieved in 30% of LBP recipients compared to 9% of those in the placebo group (benefit ratio: 3.31; $p < 0.005$). Most of this effect was due to CTV-05 colonization, although native *L. crispatus* strains were also present and increased over time. Inflammatory cytokines decreased in both arms after MTZ, but returned to baseline in the placebo group. Successful *L. crispatus* colonization was associated with pre-MTZ microbiota composition, baseline inflammatory cytokine profiles, post-MTZ total bacterial load, and selected clinical and behavioral variables. These findings elucidate LBP effects on vaginal microbiota and identify predictors of treatment success, informing strategies to develop more effective interventions to improve womens health.

36 **Introduction**

37 Bacterial vaginosis (BV), a vaginal syndrome characterized by *Lactobacillus*-deficient vaginal microbiota,
38 affects 23-29% of women of reproductive age globally, with an estimated annual economic burden of
39 $4.8 billion worldwide[1,2]. BV symptoms include vaginal discharge, malodor, pain, and itching, leading to
40 significant impairments in quality of life, self-esteem, and sexual function[3,4]. In addition, BV is linked to
41 mucosal inflammation and increased risk for numerous adverse health outcomes, such as HIV
42 acquisition, sexually transmitted infections, preterm birth, human papillomavirus (HPV) infection, and
43 cervical cancer[5–10]. While BV occurs globally, it disproportionately affects those with lower socioeconomic
44 status and members of racial or ethnic minority groups across diverse settings[1,11–13]. Development of
45 effective BV treatments is therefore a key objective to improve women's health worldwide[14].

46 Current first-line therapy for BV consists of oral or intra-vaginal antibiotics such as metronidazole (MTZ),
47 which target many species within the diverse anaerobic bacterial communities characteristic of BV[2,14]. In
48 most cases, MTZ reduces abundance of BV-associated anaerobes and leads to emergence of bacterial
49 communities dominated by *Lactobacillus* species (which are intrinsically MTZ-resistant)[15], but BV
50 frequently recurs after treatment. An Australian study of women with symptomatic BV found that 58%
51 experienced recurrent BV (rBV) within 1 year of MTZ therapy, while a US trial that enrolled women with
52 symptomatic BV and a prior history of post-treatment recurrence found that >75-80% experienced rBV
53 within 16 weeks of treatment[16,17]. It is hypothesized that the incomplete efficacy of MTZ often results from
54 a failure to eradicate BV-associated bacterial communities and/or from their post-MTZ replacement with
55 *Lactobacillus* species prone to reverting to BV[15]. Studies have shown that *Lactobacillus iners* is
56 associated with an increased risk of transition to BV-like states[18–20] and with higher rates of adverse
57 health outcomes[6,21–24]. MTZ treatment frequently results in establishment of vaginal microbiota dominated
58 by *L. iners* rather than *L. crispatus* [25–30], supporting the hypothesis that BV therapies which preferentially
59 promote *L. crispatus* over *L. iners* may improve treatment outcomes and promote vaginal health[15,31,32].

60 New strategies to enhance *L. crispatus* colonization during BV treatment are in various stages of
61 development, including vaginal microbiome transplants, adjunctive therapies that selectively inhibit *L.*
62 *iners* and/or promote *L. crispatus* growth, and *L. crispatus*-containing live biotherapeutic products
63 (LBPs)[31–38]. The most advanced LBP in development is LACTIN-V, a vaginally-administered LBP
64 containing the *L. crispatus* strain CTV-05, and the only LBP tested in large-scale clinical trials[36,39]. Cohen
65 and colleagues recently reported results of a phase 2b multi-center, randomized, placebo-controlled,
66 double-blinded study showing that participants who received 11 weeks of intravaginal LACTIN-V after a
67 5-day course of intravaginal MTZ developed rBV at lower rates than placebo recipients[36]. Benefits from
68 LACTIN-V were observed at both week 12 (approximately 1 week after completing therapy; relative risk
69 of rBV = 0.66) and week 24 (approximately 13 weeks after completing therapy; relative risk of rBV =
70 0.73). However, rBV rates remained high even in the LBP arm, with 30% of recipients experiencing rBV
71 by week 12 and 39% experiencing recurrence by week 24 in the intention-to-treat analysis. In prior
72 reports, rBV was characterized using clinical measures, but comprehensive molecular analysis of vaginal
73 microbiota composition and factors associated with colonization were not assessed.

74 Here we characterize the effects of LACTIN-V on vaginal microbiota composition and identify correlates
75 of successful colonization by analyzing vaginal microbiota composition, bacterial strain dynamics,
76 cytokine profiles, and demographic/behavioral parameters of LACTIN-V phase 2b trial participants[36]. We
77 find that the reduction in rBV among LBP recipients corresponded to >3-fold higher rates of *L. crispatus*-
78 dominant colonization, but only 30% of recipients achieved *L. crispatus*-dominant vaginal microbiota at
79 week 12, consistent with the observed incomplete clinical efficacy. Microbiota trajectory and strain
80 dynamics revealed CTV-05 accounted for the majority of *L. crispatus* colonization among LBP recipients,
81 though endogenous strains increased over time and sometimes displaced CTV-05. We further describe
82 the effects of LBP treatment and microbiota composition on vaginal immune markers, and show that pre-
83 MTZ microbiota composition, baseline inflammatory cytokine profiles, post-MTZ total bacterial load, and
84 selected clinical/behavioral variables are associated with LBP treatment success. These results show

how an *L. crispatus* LBP alters vaginal microbiota composition to improve BV treatment efficacy while identifying factors linked to LBP success that can guide development of future therapies to promote more optimal vaginal microbiota communities and improved women's health outcomes.

## Results

### Study design and participant characteristics

Women aged 18 to 45 years with BV completed five days of standard intravaginal MTZ therapy and were then randomized 2:1 to receive intravaginal LACTIN-V (Osel, Inc.) or placebo as previously described[36]. Enrollment occurred at four U.S. sites. LACTIN-V is a powder formulation containing the live *L. crispatus* strain CTV-05, administered via prefilled, single-use vaginal applicators at a dose of $2x10^9$ colony-forming units (CFU). The placebo contained the same inactive ingredients without bacteria and was visually indistinguishable. BV diagnosed at the baseline "pre-MTZ" screening visit required at least three of four Amsel criteria and a Nugent score of ≥4[40,41]. Participants received five days of intravaginal MTZ gel within 30 days of diagnosis, and then were seen at a "post-MTZ" visit within 48 hours of completing antibiotics for randomization to LBP or placebo. The first treatment dose was clinician-administered at the post-MTZ visit, then participants self-administered doses daily for four consecutive days, followed by twice weekly dosing for 10 weeks (ending at week 11 post-randomization; **Figure 1A**). Clinician-collected vaginal swabs were obtained at the pre-MTZ and post-MTZ visits prior to randomization, and at weeks 4, 8, 12, and 24 post-randomization. Detailed demographic, clinical, and behavioral data showed no notable differences between arms[36]. The trial enrolled and randomized 228 participants (152 in the LBP arm and 76 in the placebo arm); samples from 213 of these participants (142 in the LBP arm and 71 in the placebo arm) were available for this analysis, representing a total of 1,156 unique study visits.

106 **LBP Effects on *L. crispatus* and total *Lactobacillus* colonization**

107 Bacterial microbiota composition was determined by bacterial 16S V4 ribosomal RNA (rRNA) gene
108 sequencing. Four samples were excluded due to technical failures of PCR amplification and sequencing
109 ($<10^3$ processed reads per sample). Of the remaining 1,152 samples (**Table S1, Figure S1A**), the median
110 number of analyzable reads per sample was 31,177 (IQR 23,774-41,251). No significant differences in
111 microbiota composition were observed between study arms at either the pre-MTZ or post-MTZ visits
112 (PERMANOVA $p = 0.63$ and $p = 0.14$, respectively; **Figure S1B-C, SI**).

113 To assess microbiota impacts of LBP treatment, we defined two outcome parameters based on
114 microbiota proportional composition: ≥50% relative abundance of *L. crispatus* ("*L. crispatus*-dominant")
115 and ≥50% summed relative abundance of *Lactobacillus* genus ("*Lactobacillus*-dominant", including *L.*
116 *crispatus*). The primary microbiota endpoint for this analysis was establishment of an *L. crispatus*-
117 dominant vaginal community at week 12, the timepoint corresponding to the trial's primary clinical
118 endpoint[36]. Secondary microbiota endpoints were *L. crispatus*-dominance at week 24 and total
119 *Lactobacillus*-dominance at weeks 12 or 24. Almost all participants in both treatment and placebo arms
120 had non-*Lactobacillus*-dominant microbiota (<50% *Lactobacillus*) at the pre-MTZ screening visit,
121 consistent with the fact that all had met criteria for clinical BV (**Figure 1B**). The majority in both arms
122 transitioned to *Lactobacillus*-dominance at the post-MTZ visit that was largely driven by high relative
123 abundance of *L. iners* (**Table S2**). Only one participant in each arm exhibited *L. crispatus*-dominant
124 colonization at the post-MTZ visit (**Figure 1B**). Microbiota composition of the two arms diverged after
125 randomization, with 30% of LBP recipients (n=37) compared to only 9% of placebo recipients (n=5)
126 achieving *L. crispatus*-dominant colonization at week 12 (the primary endpoint), resulting in a benefit ratio
127 of 3.4 (95% CI: 1.4 - 8.1; $p < 0.005$; **Table 1**, **Figure 1B-C**). At week 24, 35% of LBP recipients (n=39)
128 versus just 8% of placebo recipients (n=4) achieved *L. crispatus*-dominant colonization, for a benefit

129 ratio of 4.5 (95% CI: 1.7 - 11.9). The LBP did not increase rates of total *Lactobacillus*-dominant
130 colonization at week 12 compared to placebo (56% and 48% of LBP and placebo recipients, respectively;
131 benefit ratio: 1.16; 95% CI: 0.85 - 1.59), but did at week 24 (58% and 33% of LBP and placebo recipients,
132 respectively; benefit ratio: 1.76; 95% CI: 1.15 - 2.68; **Table 1**, **Figure 1B-C**).

133 We next investigated how these microbiota parameters related to the clinical diagnosis of BV by
134 comparing clinical and microbiota results for all post-randomization visits (weeks 4 and beyond, n = 729
135 visits). Among the 209 visits in which participants had ≥50% *L. crispatus* colonization, none had
136 concurrent clinical BV (**Table S3** and **Figure 1C**), and among 194 visits with <50% *L. crispatus* but ≥50%
137 total *Lactobacillus*, only 1% (n=2) had BV. However, of the 326 visits with <50% total *Lactobacillus*, 50%
138 (n=164) had clinical BV (**Table S3**). Thus, *Lactobacillus*-dominance (including *L. crispatus*-dominance)
139 was highly specific for the absence of BV, while non-*Lactobacillus*-dominance was highly sensitive but
140 less specific for BV.

141 In addition to sequencing-based microbiota composition analysis, total bacterial load in vaginal swab
142 samples was assessed via quantitative PCR (qPCR) at the post-MTZ and post-randomization visits.
143 Median bacterial load was significantly lower and more variable at the post-MTZ visit (median $10^{2.69}$
144 copies/swab; IQR $10^{0.08}$ - $10^{6.44}$) than at subsequent visits (median $10^{7.52}$ copies/swab; IQR $10^{7.09}$ - $10^{7.93}$
145 for all subsequent visits), consistent with antibiotic-mediated depletion of vaginal microbiota biomass
146 during BV treatment, followed by bacterial repopulation of the vaginal environment (**Figure 1D**). We
147 assessed whether post-MTZ microbiota composition (as determined by 16S rRNA gene sequencing) was
148 correlated with total bacterial load using a multi-table multivariate generalization of the squared Pearson
149 correlation, the RV coefficient[42,43]. This analysis revealed no significant correlation between post-MTZ
150 microbiota composition and bacterial load (RV coefficient = 0.02, *p*-value > 0.1).

151 **Microbiota composition trajectories throughout the trial**

152 To characterize microbiota trajectories with greater resolution, we summarized microbiota composition
153 using topic mixtures[44,45]. Compared to clustering or categorizing samples into community state types
154 (CSTs)[46], cervicotypes (CTs)[6], or sub-CSTs[47], this method provides probabilistic (rather than binary)
155 weightings, allowing for more accurate descriptions of sample taxonomic composition and improved
156 characterization of longitudinal dynamics[45]. In our cohort, assignment to reference CST performed poorly
157 (median Bray-Curtis dissimilarity with assigned CSTs > 0.33, **SI**), especially for *Prevotella*-dominated
158 samples (median BC dissimilarity > 0.5, **SI**), and with over 40% of samples being equally similar to two
159 or more CSTs (**SI**). To identify topics, which can be interpreted as bacterial subcommunities (*i.e.,*
160 consortia of bacterial taxa that co-occur with each other or with other taxa), and estimate their proportions
161 in each sample, we fitted a latent Dirichlet allocation (LDA) model (a Bayesian "topic model")[48] to the
162 taxonomic counts. We adapted a previously described approach[45] in which topics were constrained to be
163 fully composed of either *Lactobacillus* or non-*Lactobacillus* species. Four non-*Lactobacillus* topics were
164 inferred from the data (**Figure S2A, B**) and we defined four *Lactobacillus*-dominated topics, including
165 three exclusively composed of a single *Lactobacillus* species (*L. crispatus*, *L. iners*, and *L.*
166 *jensenii*/*mulieris*) and one composed of a mixture of the remaining *Lactobacillus* species (**Figure S2C**).
167 **Figure 2A** shows inferred composition of each non-*Lactobacillus* topic, while **Figure 2B** displays topic
168 proportions for each participant throughout the trial.

169 Three non-*Lactobacillus* topics were highly prevalent and abundant in both arms at the pre-MTZ visit,
170 including topics in which the predominant taxa were *Candidatus* Lachnocurva vaginae (BVAB1),
171 *Gardnerella swidsinskii/leopoldii*, and *Prevotella amnii* (**Figure 2C** and **S2D**). Microbiota composition
172 shifted substantially at the post-MTZ visit (**Figure 2D**), where besides high *L. iners* relative abundance,
173 the non-*Lactobacillus* topic with the highest relative abundance was the topic in which *Gardnerella*
174 *swindsinskii/leopoldii* was predominant (**Figure 2C** and **S2D**). Another major shift in microbiota
175 composition occurred between the post-MTZ visit and the week 4 visit, which was larger in the LBP arm

176 (median pairwise Bray-Curtis dissimilarity: 0.81; IQR: 0.50 - 0.97) than the placebo arm (median Bray-
177 Curtis dissimilarity: 0.58; IQR 0.41 - 0.80), driven primarily by increased *L. crispatus* abundance among
178 LBP recipients (**Figure 2C-D** and **S2D**). Microbiota composition was more stable after week 4, with
179 median Bray-Curtis dissimilarity <0.55 at week 8 and all subsequent visits, which was comparable
180 between arms (**Figure 2D**). LBP recipients who achieved *L. crispatus*-dominant colonization had more
181 stable microbiota than their counterparts (**Figure S2E, SI**).

182 The observation that microbiota composition became more stable after week 4 was also supported by
183 longitudinal patterns in microbiota categories. Among 115 participants with available data from both week
184 4 and week 12 visits, 71% (25 of 35; 95% CI: 53%-85%) of LBP recipients who achieved ≥50% *L.*
185 *crispatus* at week 12 also had *L. crispatus*-dominance at week 4 (**Figure 2B, Table S4**). Similarly, 71%
186 (27 of 38; 95% CI: 54%-84%) of LBP recipients who achieved *L. crispatus*-dominance at week 24 also
187 had *L. crispatus*-dominance at week 4 (**Figure 2B**, **Table S5**). However, early *L. crispatus*-dominant
188 colonization did not guarantee persistence, as only 49% (25 of 51) and 57% (27 of 47) of LBP recipients
189 with *L. crispatus*-dominance at week 4 retained it at weeks 12 and 24, respectively. By contrast, among
190 38 LBP recipients with non-*Lactobacillus*-dominant microbiota at week 4, 79% remained non-
191 *Lactobacillus* dominant at week 12 compared to just 10.5% each with *L. crispatus*-dominance or other
192 *Lactobacillus*-dominant colonization (**Table S4**). Thus, microbiota communities established early tended
193 to persist and early *Lactobacillus*-dominance – particularly *L. crispatus*-dominance – was strongly linked
194 to ongoing *Lactobacillus*-dominance.

195 **Metagenomic identification of the CTV-05 strain and assessment of *L. crispatus* strain dynamics**

196 The observation that LBP treatment promoted *L. crispatus* colonization prompted us to examine what
197 fraction of *L. crispatus* observed in LBP recipients represented the CTV-05 strain versus non-LBP native
198 strains. We used metagenomic sequencing to assess *L. crispatus* strain dynamics, with strain genotypes
199 and proportions inferred using StrainFacts[49]. In a separate analysis, simulations and experimental spike-

200 in data showed that StrainFacts performs well at inferring LBP (including CTV-05) strain genotypes and
201 proportions in samples with ≥5% overall relative abundance of *L. crispatus*[50]. In the LACTIN-V trial
202 samples, *L. crispatus* strain inference was successful in 313 samples, identifying 24 genotypically distinct
203 strains with at least 10% fractional strain abundance in at least one sample. To determine which strain
204 represented CTV-05, we generated a closed assembly of the CTV-05 genome, which nearly perfectly
205 matched the StrainFacts genotype of a widely prevalent inferred strain within the metagenomic dataset
206 (Jaccard similarity >0.999). Among 57 samples with inferred *L. crispatus* strain composition from placebo
207 recipients (any visit) or from LBP recipients prior to LBP administration, StrainFacts inferred CTV-05
208 presence in just 5 total samples from 5 unique participants (**Figure 3A**). This result suggested our strain
209 inference approach had a low false positive CTV-05 detection rate; we cannot rule out that some "false
210 positives" represented native strains with high genotypic similarity to CTV-05. Collectively, these results
211 support that CTV-05 detection was achieved with high accuracy in sample metagenomes.

212 To further characterize fidelity of the strain-tracing approach, we analyzed inference results for native *L.*
213 *crispatus* strains, supplemented by targeted bacterial isolations and genome sequencing to
214 experimentally test bioinformatic predictions. Most participants in whom a native strain was inferred
215 exhibited colonization by only a single native strain at any point during the study, with a few participants
216 colonized by two or three native strains (**Figure 3B**). Since StrainFacts inferences are performed blinded
217 to whether samples are derived from the same participant[49,50], consistent detection of the same 1-3 native
218 strains in multiple samples from the same participant additionally supported validity of the inferences. We
219 also performed targeted bacterial isolations of *L. crispatus* from a subset of samples inferred to contain
220 CTV-05, one or more native strains, or a mixture of CTV-05 and native strains. The resulting isolates
221 were highly genotypically similar to inferred strains from the same samples, including both CTV-05 and
222 native strains (results for an example participant shown in **Figure 3C-E**, with additional participants

223 detailed in **Figure S3A**). These experimental results further validated our metagenomic strain inference
224 approach.

225 We examined *L. crispatus* strain dynamics by classifying samples with inferred strain data into three
226 categories: samples with >90% CTV-05 fractional strain abundance ("High-CTV-05"), samples with 10-
227 90% CTV-05 ("Mixed"), and samples with <10% CTV-05 ("Low-CTV-05"; **Figure 3A**). These thresholds
228 were defined based on simulations to determine parameters maximizing reliability of strain detection[50].
229 At each post-randomization timepoint, the majority of LBP recipients with analyzable *L. crispatus* strains
230 had high-CTV-05 strain abundance, but the proportion with high-CTV-05 or mixed strains decreased over
231 time, while the proportion with high native *L. crispatus* strain abundance (*i.e.*, low-CTV-05) increased
232 (**Figure 3A**). At week 4, 96.1% (n=74) of LBP recipients with ≥5% *L. crispatus* had high-CTV-05 or mixed
233 strains, while just 3.9% (n=3) had high native strains. However, by week 24 only 63.2% (n=31) had high-
234 CTV-05 or mixed strains while those with high native strains increased to 36.8% (n=18). To characterize
235 this phenomenon in greater detail, we examined CTV-05 fractional strain abundance for each pair of
236 consecutive post-randomization visits (**Figure 3F-G**). Among 144 visits with high-CTV-05, two main
237 outcomes were observed at the next visit: 68% (n=98) maintained high-CTV-05 and 26% (n=38)
238 transitioned to <5% total *L. crispatus* colonization (strain composition undetermined). Among the 18 visits
239 with high native strain abundance, 61% (n=11) retained high native strain abundance at the next visit and
240 none transitioned to CTV-05 dominance. Interestingly, among 23 visits with mixed CTV-05/native strain
241 composition, only one (4%) transitioned to high-CTV-05, while 39% (n=9) remained mixed and 35% (n=8)
242 transitioned to high native strain abundance, including some transitions to high native strain abundance
243 that occurred while participants were still receiving LACTIN-V (**Figure S3B**). These results show CTV-05
244 was frequently the sole or dominant *L. crispatus* strain in LBP recipients, but when native strains
245 dominated or co-occurred with CTV-05, they often replaced CTV-05 at subsequent visits but were almost
246 never replaced by it.

247 **Intervention effects on vaginal inflammation**

248 We assessed the effects of MTZ and LBP treatment on vaginal mucosal immune state and inflammation
249 by measuring cytokine and chemokine concentrations in vaginal swab eluates using a previously
250 described custom Luminex assay[6,45]. Concentrations of 18 cytokines and chemokines were log-
251 transformed for variance stabilization and imputed when outside their respective limits of quantification
252 (**Figure S4A**). Concentrations of all chemokines and cytokines were strongly correlated, with the first
253 principal component (PC1) accounting for 50% of the total variation (**Figure S4B**). This phenomenon
254 suggested a size-effect[51] that we attributed to the (unmeasured) variation in biomass collection between
255 swabs, which was addressed through PC1-subtraction (**SI**). Seven cytokines were excluded from
256 analysis because a large proportion of values were outside the quantification range (**Figure S4A**).
257 Mucosal immune dynamics during treatment were determined by comparing adjusted concentrations of
258 each cytokine or chemokine from each participant's baseline (pre-MTZ) visit with concentrations at
259 subsequent visits.

260 We first examined how chemokines and cytokines with known relationships to BV and vaginal microbiota
261 composition[5,6,52,53] changed during treatment. IL-1β concentrations decreased post-MTZ in both arms,
262 while IP-10 showed the opposite pattern, consistent with previously reported pattern with BV treatment[52]
263 (**Figure 4A-B**). These effects persisted in both arms through week 12, but IL-1β and IP-10 returned to
264 pre-MTZ levels by week 24 in placebo recipients, leading to a difference of -0.39 (95% CI: -0.66 – -0.14)
265 between adjusted concentrations in the LBP versus placebo arm for IL-1β and of 0.51 (95% CI: 0.21 -
266 0.79) for IP-10. By contrast, IL-6 concentrations – which have been reported not to differ between women
267 with and without BV[52] – remained unchanged from pre-MTZ levels in both treatment arms throughout the
268 study (**Figure 4C**). Sensitivity analyses examining the data prior to adjustment for size-effect via PC1-
269 subtraction revealed findings that were qualitatively similar, but with reduced magnitude (**SI**).

270 The reversion of treatment-induced effects for IL-1β and IP-10 concentrations in placebo recipients by
271 week 24 suggested an association with total *Lactobacillus* relative abundance, which differed between
272 treatment arms at this visit (**Table 1**). We therefore examined the correlation of microbiota composition
273 (summarized by topic proportions) with mucosal cytokine/chemokine concentrations. Their RV coefficient
274 was 0.18 with p-value <0.005 (permutation test), indicating significant correlation. Similar RV coefficient
275 values were obtained when repeating analysis independently for each visit (**Figure S4C**) except for a
276 substantially lower correlation at the post-MTZ visit (where microbiota absolute abundance varied widely,
277 **Figure 1D**), suggesting microbiota-immune correlation was not driven primarily by a participant effect.
278 To characterize the microbiota-immune relationship in greater detail, we employed DiSTATIS[54], a method
279 that uses between-sample dissimilarity matrices to infer a consensus matrix across two datasets and
280 associated latent components. Projecting microbiota topic relative abundances and transformed
281 cytokine/chemokine concentrations onto this latent subspace using correlation circles revealed that the
282 first latent dimension discriminated *Lactobacillus*-dominated samples from non-*Lactobacillus*-dominated
283 samples (**Figure 4D-F**). Chemokines MIG (CXCL9), IP-10 (CXCL10), and ITAC (CXCL11) had high
284 positive correlation along the first latent dimension, indicating positive covariation with *Lactobacillus*,
285 while IL-1β, TNF-α, and IL-1α had high negative correlations, indicating positive covariation with non-
286 *Lactobacillus* species (**Figure 4E**). The second latent dimension discriminated *L. crispatus* from *L. iners*
287 but most cytokines and chemokines had little or no correlation with that component, indicating minimal
288 association of inflammatory markers with individual *Lactobacillus* species (**Figure 4E**). Most cytokines
289 and chemokines had high correlations with the 3rd and/or 4th latent components but the microbiota topics
290 did not, indicating a degree of immune variation that was microbiota-independent (**Figure 4F**). In these
291 dimensions, IFNγ and IL-17 correlated with each other but were anti-correlated with IL-6, MIP-3α, MIP-
292 1β, and MIP-1α. Notably, although IP-10 levels were previously reported to differ in a small subset of
293 LACTIN-V recipients based on whether participants were highly colonized by CTV-05 versus non-CTV-
294 05 *L. crispatus* strains (as measured by qPCR)[56], we observed no clear differences in microbiota

295 correlation with cytokine/chemokine levels (including IP-10) in analysis that distinguished CTV-05 from
296 other *L. crispatus* strains (**Figure S4D-G**).

297 **Heterogeneity in LBP treatment effect based on baseline microbiota composition**

298 We next performed exploratory *post-hoc* analyses to investigate whether differences in pre-MTZ
299 microbiota composition corresponded to differences in response to the LBP (*i.e.,* heterogeneity of
300 treatment effect). We stratified participants by their most abundant pre-MTZ taxon (aggregated at the
301 genus-level), identifying four groups for analysis: *Lactobacillus*-predominant, *Gardnerella*-predominant,
302 *Prevotella*-predominant, and *Ca.* Lachnocurva vaginae (BVAB1)-predominant. LBP treatment benefit
303 was evaluated for each group with respect to two distinct outcomes: ≥50% *L. crispatus* colonization (at
304 week 12 or 24) and BV recurrence (by week 12 or 24) (**Figure 5A**). Heterogeneity in benefit among pre-
305 MTZ microbiota groups (**Figure 5B**) was tested using an analysis of deviance comparing nested logistic
306 regression models allowing (or not) for heterogeneity and adjusting for multiple testing by controlling for
307 the false discovery rate (Methods, **SI**).

308 Analysis of the relationship between pre-MTZ microbiota groups and establishment of *L. crispatus*-
309 dominant colonization suggested some groups benefitted more from LBP treatment than others (adjusted
310 *p*-values = 0.11 at week 12 and 0.03 at week 24; **Figure 5C, D**). LACTIN-V recipients with pre-MTZ
311 predominance of *Lactobacillus*, *Gardnerella*, or *Prevotella* attained higher rates of *L. crispatus*-dominant
312 microbiota at both weeks 12 and 24 compared to their placebo counterparts, with modestly larger rate
313 differences at week 24 (**Figure 5D**). In contrast, participants with pre-MTZ *Ca.* Lachnocurva vaginae
314 (BVAB1) did not differ in *L. crispatus*-dominant colonization between LBP and placebo arms. Analysis of
315 BV recurrence also showed differences in benefit from LBP treatment based on pre-MTZ microbiota
316 (adjusted *p*-values <0.05 at week 12 and <0.01 at week 2; **Figure 5E-F**). Among LBP recipients with pre-
317 MTZ *Prevotella*-predominance, BV recurred in almost all placebo recipients by week 24, compared to

318 just over half of LBP recipients. By contrast, LBP recipients whose most prevalent taxa pre-MTZ was Ca.
319 *Lachnocurva vaginae* (BVAB1) were unique in exhibiting slightly higher absolute rates of rBV than those
320 who received placebo (**Figure 5E-F**). We used similar methods to perform a sensitivity analysis in which
321 participants were grouped based on pre-MTZ CSTs[57] or using a model-based approach relying on topic
322 relative abundances. Findings from this analysis were largely consistent with results of our predominant-
323 taxon analysis above (**Figure S5, SI**). Together, these exploratory analyses showed that benefits of LBP
324 treatment in achieving *L. crispatus*-dominance and preventing BV recurrence differed depending on pre-
325 MTZ microbiota composition, with participants who had pre-MTZ predominance of *Ca.* Lachnocurva
326 vaginae (BVAB1) exhibiting a lack of benefit compared to placebo, whereas other participants
327 experienced more favorable responses.

328 **Factors associated with achieving *L. crispatus* dominance in LBP recipients**

329 To identify factors associated with establishing *L. crispatus* dominance among LBP recipients, we
330 performed a series of multiblock partial least square discriminant analyses (MB-PLS-DA) on the
331 longitudinal LACTIN-V arm data (**Figure 6A-C**, **S6**, **S7A**). Based on the observation that early *L.*
332 *crispatus*-dominant colonization correlated with *L. crispatus* colonization at later visits (**Table S4**, **S5**), we
333 analyzed factors from prior visits that associated with the participants' microbiota category by week 4, as
334 well as separate analyses of factors associated with microbiota category at ensuing visits. We defined
335 three models corresponding to the different phases of the trial: the "initial phase" spanned from the post-
336 MTZ visit to week 4, the "continuation phase" spanned from week 4 to week 12, and the "follow-up phase"
337 spanned from week 12 to week 24 (**Figure S6A**). For each phase, factors of interest (*i.e.,* explanatory
338 variables) were grouped into 13 thematic blocks (**Figure 6A**, **Table S6**). The first block characterized
339 participant demographics, blocks 2-4 described participant baseline vaginal ecosystem (*i.e.*, pre-MTZ
340 microbiota composition and diversity, pH, cytokines concentrations), blocks 5-8 quantified the vaginal
341 ecosystem at the previous visit (*e.g.,* at the post-MTZ visit in the initial phase, when the response is week
342 4 colonization status), while blocks 9-13 characterized participant sexual behavior, douching/bleeding,

343 antibiotic use, and product adherence (**Table S6**). For each phase, MB-PLS-DA was used to evaluate
344 the ability of these variables to discriminate between the following microbiota categories at each visit
345 starting from week 4: ≥50% *L. crispatus*, ≥ 50% *Lactobacillus* but <50 % *L. crispatus*, or < 50%
346 *Lactobacillus* (see also **Figure 1B**). We also used nested models to assess the additional contribution of
347 specific blocks in discriminating colonization status (**SI**, **Figure S6A-C**).

348 In the model for the LBP arm initial phase, the most important block for discriminating week 4 colonization
349 categories was the previous (*i.e.,* post-MTZ) vaginal environment (**Figure 6A**, left panel). This block
350 included post-MTZ total bacterial load, α-diversity, and pH. Lower values of these three factors were
351 associated with higher chances of ≥50% *L. crispatus* at week 4, and were among the 5 most important
352 variables in the model (**Figure 6B-C** and **S7A**). The next most important blocks were demographics and
353 blocks characterizing participant pre-MTZ vaginal environment, including pre-MTZ vaginal pH, α-
354 diversity, cytokine concentrations, and microbiota composition (as described by topic proportions, **Figure**
355 **6A** and **S7A**). Specifically, high pre-MTZ α-diversity and pH were negatively associated with *L. crispatus*
356 colonization at week 4 (**Figure 6B**). Interestingly, pre-MTZ adjusted concentrations of the chemokine IL-
357 1β were positively associated with achieving *L. crispatus*-dominance at week 4 while pre-MTZ IP-10 and
358 MIG levels showed an opposite association (**Figure 6B**, **6D**). Self-declared race and education were the
359 most important demographic block variables, with white and more highly educated participants having
360 higher rates of *L. crispatus*-dominance (**Figure S7A**). However, race and education were highly
361 correlated in the cohort (**Figure S7B**) such that their individual contributions to explaining *L. crispatus*
362 colonization could not be clearly distinguished. While these two demographic variables were also
363 correlated with several pre-MTZ vaginal characteristics that also explained colonization such as pre-MTZ
364 α-diversity (**Figure S7C**), they still mildly contributed to model explanatory power (**Figure S6C**). The
365 remaining blocks or variables were not important for discriminating between initial phase colonization
366 categories (**Figure 6A-B**, **Figure S7A**), possibly because variables in these blocks contributed limited

367 information as overall adherence was high, use of antibiotics and douching was relatively rare, and some
368 birth control options were rare in this cohort (**SI**). In contrast, within these blocks, factors with higher
369 heterogeneity across participants such as bleeding and sexual activity showed greater variable
370 importance (**Figure S7A**).

371 In the continuation phase model for the LBP arm (from week 4 to week 12), the colonization category at
372 the previous visit was by far the most important block associated with colonization category at the
373 following visit (**Figure 6A**), consistent with higher stability of microbiota composition from week 4 to 12
374 (**Figure 2D**). While no other blocks significantly improved model performance (**Figure S6C**), individual
375 variables including sexual activity, bleeding, douching, and non-hormonal IUDs were all negatively
376 associated with high-level *L. crispatus* colonization (**Figure S7A**). In the model for the LBP follow-up
377 phase (from week 12 to week 24), the colonization category at the previous visit (*i.e.,* week 12) was again
378 strongly associated with the colonization category at week 24. However, in contrast to the previous phase,
379 sexual behavior and antibiotic use only mildly contributed in explaining week 24 colonization categories
380 (**Figure 6A**, right panel, **Figure S6C**, **S7A**).

381 Analogous analyses for placebo recipients did not show significant predictive value for either the initial
382 phase or the follow-up phase in cross-validation (**Figure S8A-C**, **S9**). The placebo continuation phase
383 model had modest predictive value, with microbiota category at the previous visit serving as the best
384 predictor of microbiota category at the next visit (**Figure S8A-C**, **S9**).

385 **Discussion**

386 Treatment with vaginal live biotherapeutic products (LBPs) offers significant promise to improve health,
387 but mechanisms, correlates, and strain dynamics of LBP colonization and efficacy remain incompletely
388 understood[58]. We performed comprehensive analyses of samples and data from a randomized, double-
389 blind, placebo-controlled phase 2b trial of LACTIN-V, a single-strain *L. crispatus* LBP for prevention of
390 BV recurrence[36]. We employed microbiome sequencing, strain tracing, and immunologic characterization

391 together with multi-block analysis of biological, clinical, demographic, and behavioral parameters to
392 investigate LBP effects and correlates of treatment success. LACTIN-V treatment resulted in *L. crispatus*-
393 dominant vaginal bacterial communities in 30% and 35% of recipients at weeks 12 and 24, respectively,
394 representing 3.4- and 4.5-fold higher rates than in placebo recipients. *L. crispatus* colonization among
395 LBP recipients was substantially due to the LACTIN-V strain CTV-05, although dominance by native *L.*
396 *crispatus* strains increased over time. Microbiota trajectory analysis showed that microbial communities
397 established early frequently persisted. Achieving *Lactobacillus*-dominance – particularly *L. crispatus*-
398 dominance – at early timepoints was strongly linked to persistence of *Lactobacillus*-dominance, while
399 early non-*Lactobacillus*-dominance also tended to be maintained. In exploratory post-hoc analyses, we
400 found that the LBP's benefits differed based on baseline vaginal microbiota composition, and we
401 identified specific microbial, immune, demographic, and behavioral factors associated with high-level *L.*
402 *crispatus* colonization among LBP recipients.

403 To enhance resolution and power, we relied, for most of our analyses, on the observed relative
404 abundances of species, genera, or *de novo* topics rather than on *de novo* clusters or assignment to
405 reference community state types (CSTs). This approach is based on prior work showing that diverse
406 vaginal microbiotas do not exhibit well-defined clusters[59,60] which we also observed in this cohort. We
407 also favored taxa-based reporting to facilitate interpretation and comparison with past or future studies,
408 noting that CST definitions remain in flux as datasets expand beyond predominantly U.S. populations.

409 To elucidate mechanisms by which the LBP promoted *L. crispatus* colonization, we investigated *L.*
410 *crispatus* strain dynamics using both metagenomic analysis and cultivation-based strain characterization.
411 Metagenomic strain inferences showed the CTV-05 strain accounted for the majority of *L. crispatus*
412 colonization among LBP recipients, but native *L. crispatus* strains were also observed. Interestingly,
413 among LBP recipients with ascertainable *L. crispatus* strain composition, 96.1% had CTV-05 as their
414 dominant or co-dominant strain at week 4, but this proportion progressively declined, while the number

415 of participants with dominance by one or more native *L. crispatus* strains rose from 3.9% at week 4 to
416 36.7% at week 24. Recipients with CTV-05 strain dominance at a given visit tended to either maintain
417 CTV-05 dominance or exhibit substantial loss of *L. crispatus* at the ensuing visit. However, recipients with
418 co-dominance of CTV-05 and native strains frequently experienced replacement of CTV-05 by the native
419 strain at the next visit, but very rarely exhibited replacement of the native strain by CTV-05. Further
420 research is needed to determine whether native *L. crispatus* strains that outcompeted CTV-05 have
421 functional characteristics providing selective advantages and whether initial CTV-05 colonization
422 establishes a more permissive environment for eventual transition to native *L. crispatus* strains.

423 We also examined impacts of MTZ and LBP treatment on mucosal inflammation by measuring vaginal
424 cytokines and chemokines. Significant changes in several cytokines and chemokines were observed in
425 participants for whom treatment successfully shifted microbiota composition to *Lactobacillus*-dominance,
426 and these changes reverted in participants who shifted back to non-*Lactobacillus*-dominance. Most
427 notably, inflammatory cytokines including IL-1α, IL-1β, and TNFα increased as *Lactobacillus* abundance
428 decreased, whereas IP-10, MIG, and ITAC showed the opposite pattern, consistent with prior
429 reports[5,6,52,53]. These effects appeared primarily driven by genus-level *Lactobacillus* abundance rather
430 than a particular species. A prior study examining a subset of LACTIN-V trial participants in whom strain
431 abundance was assessed by qPCR reported that IP-10 levels were lower at week 24 in participants with
432 CTV-05 colonization than those colonized by other *L. crispatus* strains[56], but we did not observe a similar
433 association in our analysis of the full cohort. Treatment-induced cytokine changes persisted in the LBP
434 arm at week 24 compared to placebo, but this was driven primarily by the LBP's effect in promoting higher
435 rates of *Lactobacillus*-dominance rather than a strain-specific effect of CTV-05.

436 Our *post-hoc* analysis of treatment outcomes showed LACTIN-V's incomplete efficacy in achieving high-
437 level *L. crispatus* colonization and preventing BV recurrence was linked to differences in pre-MTZ
438 microbiota composition. Stratifying participants by their predominant bacterial genus at the pre-MTZ visit

439 revealed between-group differences in achieving *L. crispatus*-dominance at week 24 and in preventing
440 rBV by both weeks 12 and 24. Most prominently, these analyses showed a particular benefit from the
441 LBP in preventing BV recurrence among participants with pre-MTZ *Prevotella*-predominance, whereas
442 participants with pre-MTZ *Ca.* Lachnocurva vaginae (BVAB1)-predominance uniquely exhibited a trend
443 toward higher BV recurrence rates with LBP treatment and little or no benefit from the LBP in achieving
444 *L. crispatus*-dominance. The reasons for these patterns are unclear, but may reflect greater competitive
445 ability or MTZ resistance in *Ca.* Lachnocurva vaginae or its co-occurring species[61,62]. Since *Ca.*
446 Lachnocurva vaginae remains uncultured[63,64], experimentally testing its antimicrobial susceptibility and
447 ability to compete with other species is currently infeasible, but our results highlight its cultivation and
448 phenotypic characterization as key research priorities. However, we emphasize that these results
449 showing pre-MTZ microbiota effects on LBP efficacy are based on exploratory analyses of a relatively
450 small study cohort, which can introduce arm imbalances through *post-hoc* stratification. They should
451 therefore be regarded as hypothesis-generating observations that require replication and validation in
452 future studies.

453 We also performed integrated multiblock analysis of LBP recipients to identify biological, clinical,
454 demographic, and behavioral correlates of *L. crispatus*-dominant colonization and other microbiota
455 outcomes in LBP recipients. Low total bacterial load, low vaginal pH, and low microbiota α-diversity at
456 the post-MTZ visit were associated with *L. crispatus*-dominant colonization. Low pre-MTZ vaginal
457 concentrations of MIG and IP-10 and high concentrations of IL-1β were also associated with *L. crispatus*-
458 dominance at week 4 – an unexpected finding given their opposite correlations with *Lactobacillus*
459 abundance during concurrent visits. The explanation for this observation is unclear, but may involve a
460 more vigorous pre-MTZ mucosal immune response helping to clear BV-associated bacteria, presence of
461 inflammatory but MTZ- or LBP-responsive bacteria in some participants at baseline, or other
462 mechanisms. After week 4, the strongest predictor of a participants' microbiota category was their
463 microbiota category at the previous timepoint, indicating that microbiota composition established early

464 after LBP treatment best predicts subsequent outcomes. Demographic data including self-declared race
465 and education levels were also linked to microbiota composition at week 4 and beyond, but since race
466 and education were closely correlated and likely associated with unmeasured variables, this precluded
467 clear mechanistic interpretation. Despite evidence for sexual activity as a significant influence on BV and
468 vaginal microbiota composition[65], we did not identify a strong signal for sexual behavior as an explanatory
469 variable for microbiota composition in LBP recipients. This may be because of little variation in self-
470 reported sexual behavior throughout the trial such that effects of protected or unprotected sex may have
471 occurred early and been obscured by one of the many factors associated with early *L. crispatus*
472 colonization. It is also recognized that self-reported sexual activity in clinical trials may not be a reliable
473 measure of actual sexual activity[66–69], and reporting biases or inaccuracies can decrease power to detect
474 effects.

475 In summary, our detailed analysis of the vaginal microbiota effects of a single-strain *L. crispatus* LBP
476 reveals patterns of microbiota composition and strain dynamics underlying the clinical effects of LACTIN-
477 V. We identify key microbiota and host factors associated with treatment success and *L. crispatus*
478 colonization. If validated, these findings could help identify patients most likely to benefit from LBP
479 treatment and guide the discovery of novel therapeutic targets to enhance LBP efficacy and improve
480 women's health outcomes globally.

481 **Limitations**

482 This study has several limitations. First, samples from a few participants in the primary clinical trial were
483 not available for microbiome and cytokine analysis (samples were unavailable from 10 of 152 originally
484 reported participants in the LBP arm and 5 of 76 participants in the placebo arm). In addition, technical
485 failures of 16S rRNA gene sequencing precluded microbiota compositional analysis in four additional
486 samples, so our analysis cohort was slightly smaller than the primary trial cohort. Second, the limited size
487 of this Phase 2b study reduced statistical power, especially for heterogeneity and between-arm *L.*

488 *crispatus* colonization comparisons. Third, the study's relatively infrequent sampling schedule did not
489 permit high temporal resolution to assess microbiota and strain dynamics. Finally, although detailed data
490 were available regarding sexual, contraceptive, hygiene, and clinical parameters, participants were
491 surveyed on only a narrow range of environmental and sociodemographic variables, precluding detailed
492 investigation of factors that might help explain associations with microbiota composition.

493 **Methods**

494 **Study design and sample collection**

495 Samples analyzed in this study were obtained as part of a previously reported phase 2b, randomized,
496 double-blind, placebo-controlled trial of the *L. crispatus* LBP LACTIN-V (Osel, Inc., Mountain View, CA)
497 for prevention of rBV[36]. Use of samples was approved by the Mass General Brigham Institutional Review
498 Board (IRB Protocol #:2020P002237) as well as the UCSF Institutional Review Board (IRB Protocol#:
499 19-28337). LACTIN-V is a single-strain LBP formulated as a powder containing a preservation matrix and
500 $2x10^9$ colony-forming units (CFU) per dose of the *L. crispatus* strain CTV-05, which was isolated from a
501 human vaginal sample[36]. CTV-05 is administered using a pre-filled vaginal applicator, and was compared
502 in the trial to a placebo formulation consisting of the preservation matrix without CTV-05. The trial was
503 conducted at four centers within the USA and enrolled premenopausal, non-pregnant women aged 18-
504 45 years. Eligibility criteria were previously described[36]. Briefly, potential participants attended a
505 screening (pre-MTZ) visit at which they were determined to be eligible for the study if testing revealed
506 presence of BV as determined by both a Nugent score of 4-10 on Gram stain of a vaginal smear[41] and
507 presence of at least three of four Amsel criteria (characteristic vaginal discharge, >20% clue cells on
508 microscopy of a vaginal wet prep, vaginal fluid pH >4.5, and presence of a fishy odor upon addition of
509 10% potassium hydroxide to a vaginal specimen)[40], as well as negative testing for HIV, syphilis,
510 gonorrhea, chlamydia, trichomonas, and urinary tract infection. Women found to be eligible based on this
511 evaluation completed 5 days of intravaginal MTZ therapy within 30 days of their pre-MTZ visit (**Figure**
512 **1A, S1A)**. They then returned to the trial clinic within 48 hours of completing antibiotics (post-MTZ visit)
513 and were randomized in a 2:1 ratio to receive either LBP or placebo after providing written informed
514 consent. The first dose of LBP or placebo was clinician-administered at the randomization (post-MTZ)
515 visit, then doses were vaginally self-delivered daily for the next four days, then twice weekly for ten
516 additional weeks. In-person study visits were scheduled 4, 8, 12, and 24 weeks after randomization, at
517 which vaginal swabs were collected and stored (details below) and clinical report forms (CRFs) were

518 completed. In addition, two phone visits were planned at week 16 and 20 during which a subset of the
519 clinical report forms were filled to capture information on adverse events, menstruation, concomitant
520 medication use, and sexual behavior protected or unprotected by condoms. Participants who desired
521 additional in-person visits were invited to present to the clinics. Swabs and CRFs were collected at these
522 additional visits.

523 Clinician-collected vaginal swab samples were obtained via speculum exam at in-person study visits.
524 Two types of swabs were collected in parallel for analysis[36]. One set of swabs was collected at all in-
525 person visits including the pre-MTZ (screening) visit using the Starplex™ Scientific Multitrans™
526 Collection and Transportation System (Starplex™ Scientific S1600), which comprises a plastic-shaft
527 Dacron™-tipped swab stored in a glass bead-containing transport medium consisting gelatin (5.0 g/L),
528 sucrose (68.46 g/L), glutamic acid (0.70 g/L), HEPES sodium salt (3.4 g/L), modified Hank's balanced
529 salts (9.8 g/L), sodium bicarbonate (0.35 g/L), bovine serum albumin (10 g/L) and the antimicrobial agents
530 vancomycin (0.1 g/L), amphotericin B (2.5 mg/L), and colistin (0.015 g/L) at a pH of 7.2-7.8. The other
531 set of swabs was collected at the post-MTZ (randomization) visit and all subsequent visits in the ESwab®
532 Liquid Based Collection and Transport System (Copan ESwab 480C®). Samples were stored at room
533 temperature for 1-4 hours after collection, then frozen at -80°C.

534 Microbiota sequencing, bacterial isolation, and cytokine analysis was performed on samples stored using
535 the Starplex™ system. Samples were thawed on ice, vortexed at maximum speed for 5 seconds, then
536 the swabs were removed from the transport media and media was divided into aliquots and re-frozen at
537 -80°C. Subsequent processing was performed as described below. Measurement of bacterial load via
538 qPCR was performed using swabs collected via the Copan ESwab® system.

539 **Bacterial isolations and cultivation**

540 Bacterial isolation and cultivation was performed under anaerobic conditions at 37°C in an AS-580
541 anaerobic chamber (Anaerobe Systems) with an atmosphere of 5% carbon dioxide, 5% hydrogen, and
542 90% nitrogen (Airgas, Inc.). All culture media was pre-reduced prior to use by being placed in the
543 anaerobic chamber overnight. Bacteria were isolated and cultivated on solid media including
544 *Lactobacillus* MRS agar (Hardy Diagnostics, #G117), Columbia Blood Agar ("CBA", Hardy Diagnostics,
545 #A16), or CDC Anaerobe Laked Sheep Blood Agar with Kanamycin and Vancomycin ("LKV", BD BBL™
546 Prepared Plated Media, #221846). Known *L. crispatus* strains and not-yet-identified isolates obtained on
547 *Lactobacillus* MRS agar were expanded by culture in liquid media consisting of *Lactobacillus* MRS broth
548 (BD #288130) prepared according to manufacturer instructions. Isolates obtained on CBA agar or LKV
549 agar were expanded in liquid media consisting of either Wilkins-Chalgren Anaerobe Broth (Thermo
550 Scientific™ Oxoid™, #CM0643B; prepared according to manufacturer instructions) or of NYCIII broth
551 (American Type Culture Collection (ATCC) medium 1685), whichever produced better growth. NYCIII
552 broth was prepared using a slightly modified version of the standard ATCC protocol[34]. Pre-media
553 consisted of 4 g/L HEPES (Fisher Scientific, #BP310-500), 15 g/L proteose peptone no. 3 (BD
554 Biosciences, #BD 211693), and 5 g/L sodium chloride in 875 ml distilled water, which was pH-adjusted
555 to 7.3 and autoclaved on liquid protocol at 121°C for 15 minutes, then cooled and stored at 4°C. One day
556 before use, complete NYCIII broth was prepared from the autoclaved, cooled pre-media by adding
557 dextrose (from a stock of 3 g per 45 ml; Fisher Chemical™, #D16-500) at 7.5% v/v, yeast extract solution
558 (Gibco, #18180-059) at 2.5% v/v, and heat-inactivated horse serum (Gibco, #26050070) at 10% v/v, then
559 sterilized by passage through a 0.22 μm vacuum filter.

560 To establish a genome sequence for the CTV-05 strain, a cryopreserved pure culture of CTV-05 was
561 obtained from Osel, Inc. The strain was streaked for isolation on *Lactobacillus* MRS agar and cultured
562 for 48 hours, then a single colony was picked into *Lactobacillus* MRS broth and incubated for 20 hours.

563 The broth culture was harvested by centrifugation to obtain bacterial pellets for genomic DNA extraction
564 and sequencing.

565 Bacterial isolations were performed from twelve selected trial samples (see **Figure 3C-E**, **S3A**) using a
566 modification of previously described methods[34]. Since samples had been collected into Starplex™
567 transport medium containing antibiotics (see above), the samples were thawed on ice, immediately
568 diluted into pre-reduced Dulbecco's Phosphate Buffered Saline ("PBS", Millipore Sigma, #D8537) at 1:12
569 v/v, centrifuged for 10 minutes at 10,000 rcf, then supernatant was removed. Pellets were re-suspended
570 in PBS and re-centrifuged with removal of supernatant two more times, then resuspended in PBS, diluted
571 in serial 10-fold dilutions, and 100 $\mu$l aliquots from each dilution were plated evenly on MRS, LKV, and
572 CBA agar in parallel. Plates were incubated for 7 days and multiple examples of each distinct colony
573 morphology from each sample were picked and subcultured onto solid media of the same type as the
574 source media, with an emphasis on colonies from MRS agar with characteristic *L. crispatus* morphology
575 (e.g., **Figure 3D**). After sub-culture for 3-7 days, colonies of the subcultured bacteria were picked into
576 MRS broth (for colonies isolated on MRS agar) or into both NYCIII broth and Wilkens-Chalgren broth in
577 parallel and incubated for 1-4 days, depending on growth rate. The resulting liquid cultures were then
578 cryopreserved, with aliquots of each culture centrifuged and pellets saved for genomic DNA extraction
579 and sequencing (see below).

580 **Nucleic acid extraction for short-read sequencing**

581 Total nucleic acids (TNA) extraction from cervicovaginal swabs for microbiota profiling was performed via
582 a phenol-chloroform method, which includes a previously described bead beating process to disrupt
583 bacteria[70] and modified for processing in 96-well plate format (Phenol:Chloroform:IAA, 25:24:1, pH 6.6,
584 Invitrogen, #AM9730, which has since been discontinued; Sodium Dodecyl Sulfate 20% Solution, Fisher
585 Scientific, #BP1311-200; EDTA, Invitrogen, #AM9260G; 2-Propanol, Sigma, #I9516-500ML; 3M Sodium
586 Acetate, pH 5.5, Life Technologies, #AM9740). Aliquoted samples were thawed on ice, then TNA

587 extraction was performed using 200uL of well-mixed Star media. The extracted TNA sample was eluted
588 into 80uL of TE buffer (Promega, #V6321).

589 To extract bacterial genomic DNA (gDNA) for genome sequencing of cultured bacterial strains, each
590 isolated strain was streaked on the indicated solid media and a single, clonal colony was picked into broth
591 culture and incubated in static culture under anaerobic conditions for between 18 and 120 hours
592 (depending on strain growth kinetics). Cultures were centrifuged and gDNA was extracted from the pellets
593 using a plate-based protocol including a bead beating process and combining phenol-chloroform
594 isolation[70] with QIAamp 96 DNA QIAcube HT kit (Qiagen, # 51331) procedures.

595 **Bacterial 16S ribosomal RNA (rRNA) gene amplification and sequencing**

596 Bacterial microbiota taxonomic composition in cervicovaginal samples was determined by sequencing
597 the V4 region of the bacterial 16S rRNA gene. The V4 region was amplified via polymerase chain reaction
598 (PCR) using the primer set 515F/806R at 200 pM each (515F primer sequence
599 5'- AATGATACGGCGACCACCGAGACGTACGTACGGTGTGCCAGCMGCCGCGGTAA-3' and
600 barcoded 806R primer sequence 5'-
601 CAAGCAGAAGACGGCATACGAGATXXXXXXXXXXXXAGTCAGTCAGCCGGACTACHVGGGTWTCT
602 AAT-3', in which the underlined sequences in each primer represent the regions of complementarity to
603 5' and 3' ends of the V4 region of the bacterial 16S rRNA gene, respectively, and the barcode positions
604 in the 806R primer are indicated by X; IDT), with the 806R primers barcoded for multiplexing[34,71]. PCR
605 was performed in 25 µl reactions containing 1X Q5 reaction buffer (NEB, #B9027), 0.2 mM of dNTPs
606 (NEB, #N0447), 0.2 µM of each primer, 0.5 unit of Q5 high-fidelity DNA polymerase (NEB, #M0491), and
607 2 µl of the TNA sample. PCR was performed in triplicate for each sample in the following program: 98°C
608 for 30 seconds, followed by 30 cycles of 98°C for 10 seconds, 60°C for 30 seconds, and 72°C for 20
609 seconds, followed by a final extension at 72°C for 2 minutes. The triplicate PCR reactions for each sample
610 were combined and amplicon production and size were confirmed on an agarose gel. Negative controls

611 with PCR-quality water (Invitrogen, #10977) as a template were amplified in parallel for each primer
612 barcode mix and assessed in parallel by gel electrophoresis to confirm absence of contamination and
613 non-specific amplification. PCR products were pooled, with the amount for each sample semi-
614 quantitatively adjusted based on its gel band intensity, then purified with a QIAquick PCR purification kit
615 (Qiagen, #28104) and quality controlled with the Qubit™ 4 Fluorometer (Invitrogen #Q33226), and
616 TapeStation (Agilent Technologies, 4200 TapeStation). Libraries were mixed with 10% PhiX and single-
617 end sequenced on an Illumina MiSeq using a 300-cycle v2 kit (Illumina, #MS-102-2002) employing the
618 custom Earth Microbiome Project sequencing primers (Read 1 sequencing primer sequence: 5'-
619 ACGTACGTACGGTGTGCCAGCMGCCGCGGTAA-3'; read 2 sequencing primer sequence: 5'-
620 ACGTACGTACCCGGACTACHVGGGTWTCTAAT-3'; index sequencing primer sequence:
621 5'- ATTAGAWACCCBDGTAGTCCGGCTGACTGACT-3'; IDT)[71]. Negative controls for TNA extractions
622 and PCRs were included in each sequencing library. Study samples were sequenced in a total of six
623 libraries. Samples with read counts < 10,000 in initial libraries were re-amplified and re-pooled into
624 subsequent libraries and data from the run producing the highest number of reads for each sample (if the
625 sample was sequenced multiple times) were selected for subsequent analysis. Analyzable 16S rRNA
626 gene data was generated from a total of 1152 out of 1156 available trial samples, with the remaining 4
627 samples failing due to technical challenges with extraction, amplification, or sequencing.

628 **Bacterial short-read shotgun whole genome library preparation and sequencing**

629 Shotgun metagenomic and genomic libraries were prepared following a modified protocol of Baym et.
630 al[72], using the Nextera DNA Library Preparation Kit (Illumina, #20034211) and KAPA HiFi Library
631 Amplification Kit (Kapa Biosystems, #KK2602). In brief, DNA from each sample was standardized to a
632 concentration of 1ng/mL after quantification with SYBR Green (Invitrogen, #S7653), followed by
633 simultaneous fragmentation and sequencing adaptor incorporation by mixing 1ng of DNA (1 mL) with
634 1.25 ml TD buffer and 0.25 mL TDE1 provided in the Nextera kit and incubating for 9min at 55°C.
635 Tagmented DNA fragments were amplified in PCR using the KAPA high fidelity library amplification

636 reagents, with Illumina adaptor sequences and sample barcodes incorporated in primers. PCR products
637 were pooled, purified with magnetic beads (MagBio Genomics #AC-60050) and paired-end sequenced
638 on Illumina NovaSeq X with a 300-cycle kit (Psomagen, Inc.).

639 **Bacterial 16S rRNA gene sequence processing and annotation**

640 Demultiplexing of Illumina MiSeq bacterial 16S rRNA gene sequence data was performed using QIIME
641 1 version 1.9.188[73]. Mapping files created in QIIME 1 format were validated using
642 validate_mapping_file.py, then sequences were demultiplexed with split_libraries_fastq.py using
643 parameter store_demultiplexed_fastq and no quality filtering or trimming, and demultiplexed sequences
644 were organized into individual fastq files using split_sequence_file_on_sample_ids.py. Sequence reads
645 were trimmed and filtered using dada2 version 1.6.0[74], trimming at positions 10 (left) and 230 (right) using
646 the filterAndTrim function with truncQ = 11, MaxEE = 2, and MaxN = 0. Sequences were then inferred,
647 then initial taxonomy assigned using the dada2 assignTaxonomy function with the RDP training database
648 rdp_train_set_16.fa.gz (https://www.mothur.org/wiki/RDP_reference_files). Amplicon sequence variant
649 (ASV) taxonomic assignments were refined via extensive manual review. The resulting annotated
650 sequences were analyzed in R using phyloseq version 1.30.0[75] and custom R scripts. Sequence
651 processing and taxonomy assignment was performed blinded to information about participants' and
652 samples' clinical and demographic characteristics, treatments, and trial outcomes.

653 **Total bacterial load via qPCR**

654 Quantification of total bacterial load via qPCR was performed and reported as part of the initial LACTIN-
655 V clinical trial[36]. In brief, DNA extracted from samples stored in the Copan ESwab® system were amplified
656 using bacterial 16S rRNA gene primers targeting total bacteria (16S ribosomal DNA,
657 AGAGTTTGATCCTGGCTCAG, GCTGCCTCCCGTAGGAGT, 312bp). Bacterial concentration was
658 calculated using a standard curve based on serial dilutions of the CTV-05 strain as previously described[36].

659 **Assessing balance between arms at the pre- and post-MTZ visits.**

660 Since pre-intervention (*i.e.,* pre-MTZ or post-MTZ) microbiota composition may be associated with
661 differential microbiota composition post-intervention, imbalances between arms could lead to biases in
662 our primary outcome benefit ratio estimates. To assess whether significant imbalances in microbiota
663 composition existed in this cohort, we performed a PERMANOVA analysis, as implemented in the vegan
664 R package, to test whether the intervention arm (LBP *vs* placebo) explained significant variability in
665 microbiota β-diversity, computed using the Bray-Curtis dissimilarity on ASV relative abundances.

666 **Benefit Ratios**

667 Benefit ratios, and associated confidence intervals and *p*-value were computed using Wald's method as
668 implemented in the epitools R package[76].

669 **Identification of microbiota topics from 16S rRNA gene sequencing count data**

670 Microbiota topics were identified using a similar approach as in[45]. One main difference is that here,
671 *Lactobacillus* topics (i.e., topics composed exclusively of *Lactobacillus* species) were defined
672 independently from non-*Lactobacillus* topics (*i.e.,* topics composed exclusively of non-*Lactobacillus*
673 species), which were identified by fitting a Latent Dirichlet Allocation model[48] to the non-*Lactobacillus*
674 ASV counts aggregated at the species level. This was done to facilitate the interpretation of topic
675 composition and, specifically, to allow for "pure" topics for the most prevalent *Lactobacillus* species in
676 this cohort (*L. crispatus*, *L. iners*, and *L. jensenii*).

677 To determine *K*, the optimal number of non-*Lactobacillus* topics, we relied on a method called "topic
678 alignment"[77] which examines the robustness of topics across resolutions (increasing values of *K*) and
679 provides diagnostics scores that facilitate the identification of spurious topics. We selected *K* to minimize
680 the number of spurious topics (flagged by low coherence scores) and such that the number of paths
681 (collection of similar topics across resolution) in the alignment presented a plateau[77] (**Figure S2A**-**B**).

682 The estimated proportions (relative abundances) of non-*Lactobacillus* topics in each sample ($\hat{p}_{ki}$ where
683 $k$ is the topic and $i$ is the sample) were computed by multiplying the proportions estimated by the model
684 on non-*Lactobacillus* counts ($\hat{\pi}_{ki}$) by the total non-*Lactobacillus* proportions in each samples ($\widehat{\Pi}_i =$
685 $\sum_{v \in V} \quad p_{vi}$ where $p_{vi}$ is the observed proportion of ASV $v$ in sample $i$ and $V$ is the set of non-*Lactobacillus*
686 ASVs, such that $\hat{p}_{ki} = \hat{\pi}_{ki}\ \widehat{\Pi}_i$).

687 *Lactobacillus* topics were defined as follows: *Lactobacillus* species which reached 50% of a microbiota
688 composition in at least 10 samples made up their own topic, while the remaining *Lactobacillus* species
689 were grouped into a single topic ("Other *L.*") as their total prevalence and abundance was overall small
690 (**Figure S2C**). The composition of this topic was estimated from the species average prevalences in this
691 cohort. The estimation of proportions of *Lactobacillus* topics in each sample was straightforward: they
692 were computed from the proportions of the corresponding species in each sample.

693 **Isolate genome assemblies from short-read sequencing**

694 Paired-end short-read genomic sequencing data from bacterial isolates were processed through a quality
695 control and assembly pipeline. Raw reads were first trimmed for adapter sequences using Cutadapt v4.6
696 with the Nextera adapter sequence (CTGTCTCTTAT). Quality filtering was then performed using Sickle-
697 trim v1.33 with a quality threshold of Q20 and minimum read length of 50 bp after trimming. Read quality
698 was assessed using FastQC. De novo genome assembly was performed using Unicycler v0.5.0 in
699 standard mode with default parameters. Unicycler produces high-quality assemblies from short reads
700 alone by optimizing SPAdes assembly, followed by graph simplification. The resulting assemblies were
701 annotated using Bakta v1.9.4 with the Bakta database v5, which provides comprehensive bacterial
702 genome annotation including coding sequences, rRNAs, tRNAs, and other genomic features. Assembly
703 completeness and quality were evaluated using BUSCO v5.5 with the Bacteroidales lineage dataset
704 (bacteroidales_odb10), providing a measure of genome completeness based on conserved single-copy
705 orthologs.

706 **Strain CTV-05 long-read DNA extraction, sequencing, and completed genome assembly**

707 For long-read (Oxford Nanopore Technologies) genome sequencing of the CTV-05 strain, a bacterial
708 pellet was prepared from a clonal colony cultured in *Lactobacillus* MRS broth media as described above.
709 gDNA was extracted using a non-bead-beating protocol to minimize shearing of DNA fragments, with
710 extractions performed and sequenced using five parallel aliquots of the same original broth culture to
711 maximize yield and consistency. Since *L. crispatus* is known to have a thick cell wall containing surface-
712 layer (S-layer) proteins, cell pellets were resuspended with 5M lithium chloride (Molecular Dimensions
713 #MD2-100-43) and then washed with PBS to begin to degrade the cell wall. Using the manufacturer's
714 protocol for the MasterPureTM Gram Positive DNA Purification Kit (Biosearch Technologies
715 #MGP04100), the bacterial cells were then lysed, proteins and RNA were digested, and genomic DNA
716 (gDNA) was extracted. Extracted gDNA concentration was diluted 1:5 and measured using the Qubit™
717 4 Fluorometer, then DNA libraries were prepared using Oxford Nanopore Sequencing's Rapid Barcoding
718 Kit (Oxford Nanopore Technologies #SQK-RBK004; note that this product has been discontinued as of
719 March 2024). In brief, 400 ng of gDNA from five replicate extractions was barcoded, pooled, purified, and
720 then loaded onto the MinION Flow Cell using R9.4.1 chemistry (Oxford Nanopore Technologies #FLO-
721 MIN106D; note that this product has been discontinued as of July 2024) in the MinION Sequencing
722 Device (Oxford Nanopore Technologies #MIN-101B). To produce the maximum number of reads possible
723 using the Rapid Barcoding Kit, the sequencing run was continued for a full 72 hours.

724 Demultiplexed genomic long-reads from MinKNOW v2.2 were concatenated, and reads were separately
725 filtered for quality and length using Filtlong v0.2.1 (https://github.com/rrwick/Filtlong). Filtered reads were
726 subsampled to make 12 different read sets using Trycycler v0.5.3[78] and duplicate reads from each read
727 set were removed using BBMap v39.00[79]. The read sets were assembled using Flye v2.9.1[80], Minipolish
728 v0.1.3[81], Raven v1.8.1[82], and Canu v2.2[83]. Contigs from different assembly methods were clustered
729 based on similarity to generate consensus sequences and improve assembly quality using Trycycler.
730 Clusters were manually chosen and Trycycler was used to reconcile the contigs within each cluster.

731 Multiple sequence alignment and read partitioning were performed on the reconciled contigs using
732 Trycyler to understand sequence variation within each cluster and assign each read to the cluster it best
733 aligned with respectively. Trycycler was then used to generate a consensus contig sequence for each
734 cluster based on the multiple sequence alignment and read partitioning steps. Medaka v1.7.2
735 (https://github.com/nanoporetech/medaka), a tool for creating consensus sequences specifically from
736 nanopore sequence data, was used to polish the Trycycler consensus sequences. The consensus
737 sequences were then combined, after which Polypolish v0.5.0[84] was used to polish the long-read
738 sequence with Illumina short-read data generated from an aliquot of the same clonal culture of CTV-05
739 (extracted and sequenced as described above). The complete CTV-05 genome was annotated using
740 Bakta v1.7.0[85] and published online as part of this manuscript under NCBI BioProject reference number:
741 PRJNA1303956.

742 **Construction of *L. crispatus* core SNP database for strain analysis**

743 A GT-Pro database of biallelic core sites was constructed using 236 *L. crispatus* genomes using k-mers
744 with thresholds for SNP prevalence of 0.95 and minor allele frequencies of 0.02 with MAAST[50,86,87]. Then
745 k-mers for samples were counted to generate a metagenotype, or a matrix of the number of reads at
746 biallelic SNP sites for a single species[49]. This matrix was then used by StrainFacts to infer suitable allele
747 and relative abundance matrices that represent strains across all given samples[50].

748 ***L. crispatus* strain estimation in metagenomes**

749 Raw metagenomic paired-end reads from vaginal swab samples were quality-trimmed and adapter-
750 filtered using Cutadapt (v3.9)[88]. Human reads were depleted by aligning reads to the T2T-CHM13
751 reference genome using HISAT2 (v2.2.1)[89]. Processed reads were profiled using GT-Pro (v1.0.1) against
752 the custom SNP database[87]. Resulting metagenotype profiles were analyzed with StrainFacts (v0.6.0) to
753 infer strain genotypes and abundances for *L. crispatus*, excluding samples with <25% coverage of the
754 biallelic SNPs[49]. The fit was then run through a cleanup step to remove low abundance strains and strains

755 with extremely similar genotypes using sfacts cleanup_fit --abundance 0.01 --dissimilarity 0.01 --

756 discretized. Analysis was performed on samples with ≥5% overall relative abundance of *L. crispatus* as

757 determined by 16S rRNA gene sequencing based on evaluations of parameters supporting accurate
758 StrainFacts LBP strain inference[50]. *L. crispatus* strain inference was successful in 313 of 343 samples in
759 which species relative abundance exceeded the analysis threshold, while strain analysis was
760 unsuccessful in the remaining 30 samples due to failed or inadequately deep shotgun metagenomic
761 sequencing. A 10% strain proportional abundance was used as a threshold for confident strain
762 identification based on prior simulations and experimental validation[50].

763 **Strain analysis of isolate genomes and comparison to metagenomically inferred strain genotypes**
764 Isolate genomes were taxonomically identified using GTDB-Tk v2[90]. Gene-calling was performed for *L.*
765 *crispatus* isolate genomes, including the completed CTV-05 genome (see above) using Prodigal[91]. Core
766 ribosomal proteins were identified using HMMER[92], aligned using mafft[93,94], then concatenated and a
767 phylogenetic tree was constructed using fasttree[95,96], which was used to compute branch lengths to
768 identify isolates representing distinct strains and determine which isolates represented CTV-05 or
769 endogenous strains. GT-Pro[87] was then used to calculate genotypes from representative isolate reads
770 for comparison to metagenomically inferred strain genotypes, calculated based on Jaccard similarity of
771 the StrainFacts genotypes[50].

772 **Measurement of vaginal mucosal cytokines and chemokines.**

773 Cytokines and chemokines were measured using a previously described custom 20-plex High Sensitivity
774 Luminex Assay Kit from EMD Millipore that measures interferon gamma-induced protein (IP-10),
775 interleukin 8 (IL-8), interleukin 6 (IL-6), monokine induced by interferon gamma (MIG), interferon-
776 inducible T cell alpha chemoattractant (ITAC), interleukin 1 alpha (IL-1α), interleukin 1 beta (IL-1β),
777 macrophage inflammatory protein-1 alpha (MIP-1α), macrophage inflammatory protein-1 beta (MIP-1β),

778 macrophage inflammatory protein-3 alpha (MIP-3α), tumour necrosis factor alpha (TNFα), interleukin 21
779 (IL-21), interleukin 17 (IL-17), interferon gamma (IFNγ), interleukin 23 (IL-23), interleukin 12 (IL-12 p70),
780 interleukin 13 (IL-13), interleukin 10 (IL-10), interleukin 4 (IL-4), and interleukin 5 (IL-5)[6]. Reagents were
781 used as supplied by the manufacturer, except the Mixed Beads solution, detection antibody mixture, and
782 Streptavidin-phycoerythrin (Strep-PE) were diluted 3-fold (1:2 volume:volume ratio) for use. The Mixed
783 Beads were diluted in Bead Diluent, while the detection antibodies and Strep-PE were diluted individually
784 in Assay Buffer. All reagents were from a single manufacturer lot to minimize batch effects.

785 Samples were first pre-processed to remove interfering mucus and debris. In brief, 200 $\mu$L aliquots of
786 each vaginal swab supernatant were thawed on ice, vortexed for 10 seconds to resuspend, then
787 centrifuged at 1000 rcf for 15 minutes at 4°C to pellet mucous and cells. The maximum amount of
788 supernatant recoverable from each sample without disturbing the resulting pellet was then transferred to
789 a well of a 0.22 m PVDF filter plate (EMD Millipore #MSGVS2210), filtered by centrifugation at 2,451 rcf
790 for 1 hour at 4°C, then transferred to freezer-safe tubes and stored at -80°C until assayed. Samples were
791 assayed in 96-well plates as per manufacturer protocol with the addition of periodic sonication steps to
792 minimize bead clumping. Each plate assay included one blank background control, 7 standard serial
793 dilutions assayed in duplicate, two manufacturer-supplied Quality Control (QC) samples assayed in
794 duplicate, 72 experimental samples, and 4 biological control samples used as internal quality controls on
795 all plates. Batches of standards and QC samples were prepared from the kit on the day of the assay
796 according to manufacturer protocol. For each sample or standard, 25 $\mu$L each of Assay Buffer, Mixed
797 Beads, and sample were aliquoted into each plate well. After the addition of Mixed Beads, all incubation
798 steps were performed while the plate was protected from light. Plates were sonicated for 30 seconds at
799 room temperature in a bath sonicator, then incubated for 16-18 hours on a horizontal plate shaker at 600
800 rpm in 4°C. An additional 30 second sonication at room temperature was then performed. A handheld
801 plate magnet was applied to the base of the plate to retain the magnetic beads and excess sample and
802 reagents were removed via three consecutive washes using manufacturer-supplied 1X Wash Buffer.

803 Detection antibodies were added as per manufacturer protocol and plates were incubated for 1 hour at
804 room temperature on a horizontal plate shaker at 600 rpm. Next, Strep-PE reagent was added, followed
805 by a 30 minute incubation at room temperature on a horizontal plate shaker at 600 rpm. Plates were
806 washed 3 times as above using the magnet. After the final wash, 150 $\mu$L of sheath fluid was added to all
807 wells and a final 30 second sonication at room temperature was performed. Analyte concentrations were
808 measured using a FLEXMAP 3D instrument with Luminex xPONENT software.

809 **Cytokine and chemokine concentration transformations**

810 Cytokine and chemokine concentrations were log-transformed (log) to stabilize the mean-variance
811 relationship. Compounds with concentration values below the lower limit of quantification (LLOQ) were
812 imputed at half the LLOQ; those with concentration values above the upper limit of quantification (ULOQ)
813 were imputed at the ULOQ (**Figure S4A**).

814 Measurement of soluble molecules in swab samples can be complicated by a “size effect” phenomenon
815 whereby a component of between-swab variation in concentrations is due to technical differences in the
816 amount of material collected on each swab. In such situations, the first principal component (PC1), which
817 reflects the “size” of observations[51], can primarily be driven by the amount of material on the swab rather
818 than biological variation. Consistent with this size effect phenomenon, we observed that per-sample
819 cytokine/chemokine concentrations were highly collinear, with PC1 of the standardized log-transformed
820 cytokine concentrations accounting for over 50% of the total variance (**Figure S4B**) but showed no
821 substantial correlation with clinical and biological factors such as proportions of total *Lactobacillus* or of
822 *Lactobacillus crispatus*, or participants’ contraceptives (**SI**). Such size effects can be addressed by
823 subtracting PC1 from the data. We therefore performed PC1 subtraction by re-assigning scores
824 corresponding to the 1st PC to a value of 0, then transforming the data back to its original variable space
825 using the transposed rotation matrix (**SI**). Sensitivity analyses were performed to assess the impact of
826 this transformation on findings (**SI**). Finally, due to the large uncertainty regarding their distributions,

827 cytokines with values below the LLOQ in ≥60% of the samples or with values above the ULOQ in ≥30%
828 of the samples were excluded from the analysis (**Figure S4A**).

829 **Associations between microbiota composition and cytokine profiles**

830 To quantify the association between microbiota composition and cytokine profiles, we computed the RV
831 coefficient between the microbiota composition as expressed as topic proportions and cytokine
832 transformed log10-concentrations. Associated *p*-value was computed with a permutation test[97,98]. To
833 confirm that correlation between these tables was not driven by potential subject (longitudinal) effects,
834 we also computed correlation between the two tables at each visit independently. If correlations were
835 found significant, further analyses were carried out to characterize the relationship between tables.
836 Specifically, DISTATIS[55,99], as implemented in the distatisR R package, was used. This method presents
837 the advantage of estimating compromise scores (and partial residual scores) directly from dissimilarity
838 matrices such that ecological measures of (dis)similarity, such as the Bray-Curtis dissimilarity, can be
839 used for representing microbiota composition. Associations with the original variables can then be
840 assessed using correlations and displayed in correlation circles as typically done with PCA, PCoA, or
841 NMDS results. The minimum number of components used for display was chosen based on the presence
842 of an elbow in the DiSTATIS scree plot.

843 **Estimating effect heterogeneity**

844 Binary outcomes (Y: ≥50% colonization by *L. crispatus* at week 12 or 24 or absence of rBV by week 12
845 or 24) were predicted using logistic regression (logit link function) with input variables representing the
846 intervention arm (*A*: LBP or placebo), the baseline (pre-MTZ) microbiota (*V*: stratified by most prevalent
847 genus, CST, or topic proportions), and their interactions (*A:V*). In stratification analyses, strata with less
848 than two participants per arm were excluded from the analysis and visualizations. Since *Lactobacillus*
849 species other than *L. iners* had low pre-MTZ relative abundance, prior to determining fits relying on topic

850 proportions, *Lactobacillus*-dominated topics were agglomerated such that the proportion of total
851 *Lactobacillus* was considered, which improved fit convergence. The statistical significance of effect
852 heterogeneity was tested by comparing the null model (which only includes the intervention arm as
853 predictor) with the full model where pre-MTZ microbiota and interaction effects were included (analysis
854 of deviance F test). *P*-values were adjusted to account for multiple hypotheses testing using the
855 Benjamini-Hochberg procedure[100]. For the stratified analyses, CI were computed using Wilson scores
856 due to the small sample size in each stratum. When pre-MTZ microbiota composition was included as a
857 quantitative multivariate variable, counterfactual probabilities of success and associated 95% confidence
858 intervals were predicted from the logistic regression fitted model by setting the intervention arm to LBP
859 or placebo. The predicted participant-level odd ratios were computed as the ratio between predicted odds
860 of *L. crispatus* colonization at week 12 and 24 or rBV by week 12 or 24 had participants been receiving
861 LBP or the placebo.

862 **Identifying factors associated with successful *L. crispatus* colonization in intervention arm**

863 To identify demographic, clinical, behavioral, or microbiologic factors associated with successful *L.*
864 *crispatus* colonization (≥ 50%) in the intervention arm, we relied on a multiblock partial least square
865 discriminant analysis (MB-PLS-DA)[101] where the 3-category response variable indicated whether (1)
866 relative abundance of *L. crispatus* was ≥50%, (2) relative abundance of total *Lactobacillus* (any species)
867 was ≥50% but relative abundance of *L. crispatus* was <50%, or (3) the relative abundance of total
868 *Lactobacillus* was <50%. MB-PLS-DA relies on the same principles as PLS-DA but allows for explanatory
869 variables to be grouped into several thematic blocks, which enables the computation of block importance
870 indices and covariances with the response block[101,102]. The description of each block and associated
871 variables is provided in Table S6.

872 Several explanatory variables were correlated. For example, the abundances of some cytokines
873 correlated with microbiota composition (**Figure 4**), and the baseline α-diversity was lower in White
874 participants (**Figure S7C**, p-value < 0.05). We addressed these existing correlations between explanatory
875 blocks and/or variables in two different ways depending on our assumptions on the underlying correlation
876 source or cause. We either relied on nested models to evaluate the additive predictive power of specific
877 blocks (*e.g.,* demographics) that had variables correlated with microbiological blocks or used one variable
878 or one block to predict the values of another one and included the residuals instead of the observed
879 values in the model. This was indicated by the symbol (r) in the variable or block names (see **SI** for
880 details). We used this approach for the cytokine blocks whose residuals were computed using their PLS-
881 predicted abundances based on microbiota composition (**SI**). Similarly, we computed residual microbiota
882 composition, α-diversity, and pH at the previous visit such that topic proportions, α-diversity, or pH were
883 relative to those expected based on the participants' colonization status at the same visit.

884 Categorical variables such as race or birth control were included using one-hot encoding, and variables
885 were standardized. To ensure convergence of the fits in cross-validation or using the bootstrap, we added
886 Gaussian noise with very small variance ($\sigma_i{}^2 = 10^{-3} S_i{}^2$ where $\sigma_i{}^2$ is the variance of the Gaussian noise
887 for variable $i$, and $S_i{}^2$ the empirical variance of the $i^{th}$ variable) to one-hot encoded variables that had
888 few participants in some categories.

889 Given that our categorical response had three categories, we selected two latent components for the MB-
890 PLS-DA models to avoid overfitting. Further, we performed cross-validation analyses (40 random 75-
891 25% split into calibration and validation sets) and found that two latent components maximized the mean
892 average F1 score on the validation sets for all models except for the initial phase of the placebo in which
893 no variables were found to predict our response, leading to poor and unstable performances in cross-
894 validation (**Figure S6B** and **S8A**). This was consistent with the presence of an elbow in the screeplots
895 and robust to other choices of metrics such as accuracy or RMSE (**SI**). Relative cumulative block

896 importance indices were computed by dividing cumulative block importance, the BIPC as in[101], by the
897 total inertia of each block, which corresponds to the expected BIPC if all variables had a similar
898 importance (**SI**).

899 **Acknowledgments**

900 We thank members of the Vaginal Microbiome Research Consortium for helpful discussions. Funding
901 was obtained by D.S.K from the Gates Foundation (INV-033690). S.M.B. was partially supported by NIH
902 grant 1K08AI171166.

903 **Author Contributions**

904 D.S.K., S.P.H., S.M.B., and L.S. conceptualized the research with input from J.E., C.M.M., A.H., and
905 C.R.H.; D.S.K. and S.P.H. supervised the project; S.M.B., L.S., J.E., J.X., S.H., J.S., and S.P.H.
906 developed and validated methods and models; S.M.B., J.X., S.H., A.S., C.M.M., T.P.P., A.K., and F.A.H.
907 generated samples and performed experiments; L.S., S.M.B., J.E., J.S., A.H., A.K., F.A.H., and S.P.H.
908 performed data analysis; L.S., S.M.B., and D.S.K. led writing of the manuscript with contributions from
909 S.P.H., J.E., J.X., S.H., C.M.M., A.H., T.P.P., A.K., F.A.H., and C.R.H.; All authors provided critical
910 feedback on methods, results, analysis, and writing.

911 **Competing Interests**

912 C.M.M. has a financial interest in Ancilia Biosciences, a company developing a new class of Live
913 Biotherapeutics and other bacterial products. C.M.M. interests were reviewed and are managed by MGH
914 and Mass General Brigham in accordance with their conflict-of-interest policies. C.M.M. serves on the
915 scientific advisory board for Concerto Bio, has served as a consultant for Scynexis and Ancilia
916 Biosciences, and has received royalties from Up to Date. C.R.C. has served as a scientific advisor for
917 Osel, Inc, and Evvy and has stock options from both. The UCSF Conflict of Interest Committee approved
918 a plan to minimize his potential conflict of interest. T.P.P. is an employee of Osel Inc.

919 **Data and code availability**

920 Sequencing data and genome assemblies generated as part of this study are posted under NCBI
921 BioProject reference number: PRJNA1303956. Analysis scripts and SI are available on our publicly
922 available GitHub repository (https://github.com/lasy/IIb-LACTIN-V-omics-reanalysis/).

923 **References**


924 1. Peebles, K., Velloza, J., Balkus, J. E., McClelland, R. S. & Barnabas, R. V. High Global Burden and
925 Costs of Bacterial Vaginosis: A Systematic Review and Meta-Analysis. *Sex. Transm. Dis.* **46**, 304–
926 311 (2019).
927 2. Workowski, K. A. *et al.* Sexually Transmitted Infections Treatment Guidelines, 2021. *MMWR*
928 *Recomm. Rep. Morb. Mortal. Wkly. Rep. Recomm. Rep.* **70**, 1–187 (2021).
929 3. Brusselmans, J., De Sutter, A., Devleesschauwer, B., Verstraelen, H. & Cools, P. Scoping review of
930 the association between bacterial vaginosis and emotional, sexual and social health. *BMC Womens*
931 *Health* **23**, 168 (2023).
932 4. Bilardi, J. E. *et al.* The burden of bacterial vaginosis: women's experience of the physical,
933 emotional, sexual and social impact of living with recurrent bacterial vaginosis. *PloS One* **8**, e74378
934 (2013).
935 5. Anahtar, M. N. *et al.* Cervicovaginal bacteria are a major modulator of host inflammatory responses
936 in the female genital tract. *Immunity* **42**, 965–976 (2015).
937 6. Gosmann, C. *et al.* Lactobacillus-Deficient Cervicovaginal Bacterial Communities Are Associated
938 with Increased HIV Acquisition in Young South African Women. *Immunity* **46**, 29–37 (2017).
939 7. Atashili, J., Poole, C., Ndumbe, P. M., Adimora, A. A. & Smith, J. S. Bacterial vaginosis and HIV
940 acquisition: a meta-analysis of published studies. *AIDS Lond. Engl.* **22**, 1493–1501 (2008).
941 8. Hillier, S. L. *et al.* A case-control study of chorioamnionic infection and histologic chorioamnionitis in
942 prematurity. *N. Engl. J. Med.* **319**, 972–978 (1988).
943 9. Leitich, H. & Kiss, H. Asymptomatic bacterial vaginosis and intermediate flora as risk factors for
944 adverse pregnancy outcome. *Best Pract. Res. Clin. Obstet. Gynaecol.* **21**, 375–390 (2007).
945 10. Brusselaers, N., Shrestha, S., van de Wijgert, J. & Verstraelen, H. Vaginal dysbiosis and the risk of
946 human papillomavirus and cervical cancer: systematic review and meta-analysis. *Am. J. Obstet.*
947 *Gynecol.* **221**, 9-18.e8 (2019).

948 11. Allsworth, J. E. & Peipert, J. F. Prevalence of bacterial vaginosis: 2001-2004 National Health and
949 Nutrition Examination Survey data. *Obstet. Gynecol.* **109**, 114–120 (2007).
950 12. Kenyon, C., Colebunders, R. & Crucitti, T. The global epidemiology of bacterial vaginosis: a
951 systematic review. *Am. J. Obstet. Gynecol.* **209**, 505–523 (2013).
952 13. Marconi, C., Duarte, M. T. C., Silva, D. C. & Silva, M. G. Prevalence of and risk factors for bacterial
953 vaginosis among women of reproductive age attending cervical screening in southeastern Brazil.
954 *Int. J. Gynaecol. Obstet. Off. Organ Int. Fed. Gynaecol. Obstet.* **131**, 137–141 (2015).
955 14. Bradshaw, C. S. & Sobel, J. D. Current Treatment of Bacterial Vaginosis—Limitations and Need for
956 Innovation. *J. Infect. Dis.* **214**, S14–S20 (2016).
957 15. Bradshaw, C. S. & Brotman, R. M. Making inroads into improving treatment of bacterial vaginosis -
958 striving for long-term cure. *BMC Infect. Dis.* **15**, 292 (2015).
959 16. Schwebke, J. R. *et al.* Treatment of Male Sexual Partners of Women With Bacterial Vaginosis: A
960 Randomized, Double-Blind, Placebo-Controlled Trial. *Clin. Infect. Dis. Off. Publ. Infect. Dis. Soc.*
961 *Am.* **73**, e672–e679 (2021).
962 17. Bradshaw, C. S. *et al.* High recurrence rates of bacterial vaginosis over the course of 12 months
963 after oral metronidazole therapy and factors associated with recurrence. *J. Infect. Dis.* **193**, 1478–
964 1486 (2006).
965 18. Munoz, A. *et al.* Modeling the temporal dynamics of cervicovaginal microbiota identifies targets that
966 may promote reproductive health. *Microbiome* **9**, 163 (2021).
967 19. Tamarelle, J., Shardell, M. D., Ravel, J. & Brotman, R. M. Factors Associated With Incidence and
968 Spontaneous Clearance of Molecular-Bacterial Vaginosis: Results From a Longitudinal Frequent-
969 Sampling Observational Study. *Sex. Transm. Dis.* **49**, 649–656 (2022).
970 20. DiGiulio, D. B. *et al.* Temporal and spatial variation of the human microbiota during pregnancy.
971 *Proc. Natl. Acad. Sci.* **112**, 11060–11065 (2015).
972 21. van Houdt, R. *et al.* Lactobacillus iners-dominated vaginal microbiota is associated with increased

973 susceptibility to Chlamydia trachomatis infection in Dutch women: a case-control study. *Sex.*
974 *Transm. Infect.* **94**, 117–123 (2018).
975 22. Colbert, L. E. *et al.* Tumor-resident Lactobacillus iners confer chemoradiation resistance through
976 lactate-induced metabolic rewiring. *Cancer Cell* **41**, 1945-1962.e11 (2023).
977 23. Norenhag, J. *et al.* The vaginal microbiota, human papillomavirus and cervical dysplasia: a
978 systematic review and network meta-analysis. *BJOG Int. J. Obstet. Gynaecol.* **127**, 171–180
979 (2020).
980 24. Kindinger, L. M. *et al.* The interaction between vaginal microbiota, cervical length, and vaginal
981 progesterone treatment for preterm birth risk. *Microbiome* **5**, 6 (2017).
982 25. Srinivasan, S. *et al.* Temporal variability of human vaginal bacteria and relationship with bacterial
983 vaginosis. *PloS One* **5**, e10197 (2010).
984 26. Ravel, J. *et al.* Daily temporal dynamics of vaginal microbiota before, during and after episodes of
985 bacterial vaginosis. *Microbiome* **1**, 29 (2013).
986 27. Verwijs, M. C., Agaba, S. K., Darby, A. C. & Van De Wijgert, J. H. H. M. Impact of oral
987 metronidazole treatment on the vaginal microbiota and correlates of treatment failure. *Am. J.*
988 *Obstet. Gynecol.* **222**, 157.e1-157.e13 (2020).
989 28. Joag, V. *et al.* Impact of Standard Bacterial Vaginosis Treatment on the Genital Microbiota, Immune
990 Milieu, and Ex Vivo Human Immunodeficiency Virus Susceptibility. *Clin. Infect. Dis.* **68**, 1675–1683
991 (2019).
992 29. Mitchell, C. *et al.* Behavioral predictors of colonization with Lactobacillus crispatus or Lactobacillus
993 jensenii after treatment for bacterial vaginosis: a cohort study. *Infect. Dis. Obstet. Gynecol.* **2012**,
994 706540 (2012).
995 30. Ferris, M. J., Norori, J., Zozaya-Hinchliffe, M. & Martin, D. H. Cultivation-independent analysis of
996 changes in bacterial vaginosis flora following metronidazole treatment. *J. Clin. Microbiol.* **45**, 1016–
997 1018 (2007).

998 31. Zhu, M. *et al.* Vaginal Lactobacillus fatty acid response mechanisms reveal a metabolite-targeted
999 strategy for bacterial vaginosis treatment. *Cell* **187**, 5413-5430.e29 (2024).
1000 32. Nilsen, T., Swedek, I., Lagenaur, L. A. & Parks, T. P. Novel Selective Inhibition of Lactobacillus
1001 iners by Lactobacillus-Derived Bacteriocins. *Appl. Environ. Microbiol.* **86**, e01594-20 (2020).
1002 33. Lev-Sagie, A. *et al.* Vaginal microbiome transplantation in women with intractable bacterial
1003 vaginosis. *Nat. Med.* **25**, 1500–1504 (2019).
1004 34. Bloom, S. M. *et al.* Cysteine dependence of Lactobacillus iners is a potential therapeutic target for
1005 vaginal microbiota modulation. *Nat. Microbiol.* **7**, 434–450 (2022).
1006 35. Yockey, L. J. *et al.* Screening and characterization of vaginal fluid donations for vaginal microbiota
1007 transplantation. *Sci. Rep.* **12**, 17948 (2022).
1008 36. Cohen, C. R. *et al.* Randomized Trial of Lactin-V to Prevent Recurrence of Bacterial Vaginosis. *N.*
1009 *Engl. J. Med.* **382**, 1906–1915 (2020).
1010 37. Ravel, J. *et al.* Impact of a multi-strain L. crispatus-based vaginal synbiotic on the vaginal
1011 microbiome: a randomized placebo-controlled trial. *NPJ Biofilms Microbiomes* **11**, 158 (2025).
1012 38. Chetty, C. *et al.* Randomized Trial of Multi-Strain Lactobacillus crispatus Vaginal Live
1013 Biotherapeutic Products after Antibiotic Therapy for Bacterial Vaginosis: Study Protocol for
1014 VIBRANT (Vaginal Live Biotherapeutic RANdomized Trial). Preprint at
1015 https://doi.org/10.2139/ssrn.5261044 (2025).
1016 39. Hemmerling, A. *et al.* Phase 1 dose-ranging safety trial of Lactobacillus crispatus CTV-05 for the
1017 prevention of bacterial vaginosis. *Sex. Transm. Dis.* **36**, 564–569 (2009).
1018 40. Amsel, R. *et al.* Nonspecific vaginitis: Diagnostic criteria and microbial and epidemiologic
1019 associations. *Am. J. Med.* **74**, 14–22 (1983).
1020 41. Nugent, R. P., Krohn, M. A. & Hillier, S. L. Reliability of diagnosing bacterial vaginosis is improved
1021 by a standardized method of gram stain interpretation. *J. Clin. Microbiol.* **29**, 297–301 (1991).
1022 42. Robert, P. & Escoufier, Y. A Unifying Tool for Linear Multivariate Statistical Methods: The RV-

1023 Coefficient. *J. R. Stat. Soc. Ser. C Appl. Stat.* **25**, 257–265 (1976).
1024 43. Josse, J. & Holmes, S. Measuring multivariate association and beyond. *Stat. Surv.* **10**, (2016).
1025 44. Sankaran, K. & Holmes, S. P. Latent variable modeling for the microbiome. *Biostatistics* **20**, 599–
1026 614 (2019).
1027 45. Symul, L. *et al.* Sub-communities of the vaginal microbiota in pregnant and non-pregnant women.
1028 *Proc. R. Soc. B Biol. Sci.* **290**, 20231461 (2023).
1029 46. Ravel, J. *et al.* Vaginal microbiome of reproductive-age women. *Proc. Natl. Acad. Sci.* **108**, 4680–
1030 4687 (2011).
1031 47. France, M. T. *et al.* VALENCIA: a nearest centroid classification method for vaginal microbial
1032 communities based on composition. *Microbiome* **8**, 166 (2020).
1033 48. Blei, D. M., Ng, A. Y. & Jordan, M. I. Latent Dirichlet Allocation. *J. Mach. Learn. Res.* 30 (2003).
1034 49. Smith, B. J., Li, X., Shi, Z. J., Abate, A. & Pollard, K. S. Scalable Microbial Strain Inference in
1035 Metagenomic Data Using StrainFacts. *Front. Bioinforma.* **2**, (2022).
1036 50. Shih, J. *et al.* StrainFacts accurately quantifies bacterial strain abundance and dynamics in
1037 simulated and real-world microbiota samples treated with live biotherapeutic products (LBPs).
1038 *Manuscr. Prep.*
1039 51. Jolicoeur, P. & Mosimann, J. E. Size and Shape Variation in The Painted Turtle. A Principal
1040 Component Analysis. *Growth* (1960).
1041 52. Masson, L. *et al.* Defining genital tract cytokine signatures of sexually transmitted infections and
1042 bacterial vaginosis in women at high risk of HIV infection: a cross-sectional study. *Sex. Transm.*
1043 *Infect.* **90**, 580–587 (2014).
1044 53. Masson, L. *et al.* Inflammatory cytokine biomarkers of asymptomatic sexually transmitted infections
1045 and vaginal dysbiosis: a multicentre validation study. *Sex. Transm. Infect.* **95**, 5–12 (2019).
1046 54. Abdi, H., Dunlop, J. P. & Williams, L. J. How to compute reliability estimates and display confidence
1047 and tolerance intervals for pattern classifiers using the Bootstrap and 3-way multidimensional

1048 scaling (DISTATIS). *NeuroImage* **45**, 89–95 (2009).
1049 55. Abdi, H., O'Toole, A. J., Valentin, D. & Edelman, B. DISTATIS: The Analysis of Multiple Distance
1050 Matrices. in *2005 IEEE Computer Society Conference on Computer Vision and Pattern Recognition*
1051 *(CVPR'05) - Workshops* vol. 3 42–42 (IEEE, San Diego, CA, USA, 2005).
1052 56. Armstrong, E. *et al.* Sustained effect of LACTIN-V (Lactobacillus crispatus CTV-05) on genital
1053 immunology following standard bacterial vaginosis treatment: results from a randomised, placebo-
1054 controlled trial. *Lancet Microbe* **3**, e435–e442 (2022).
1055 57. France, M. T. *et al.* VALENCIA: a nearest centroid classification method for vaginal microbial
1056 communities based on composition. *Microbiome* **8**, 166 (2020).
1057 58. Bradshaw, C. S. *et al.* Bacterial vaginosis. *Nat. Rev. Dis. Primer* **11**, 43 (2025).
1058 59. Symul, L. *et al.* Sub-communities of the vaginal microbiota in pregnant and non-pregnant women.
1059 *Proc. R. Soc. B Biol. Sci.* **290**, 20231461 (2023).
1060 60. Lebeer, S. *et al.* A citizen-science-enabled catalogue of the vaginal microbiome and associated
1061 factors. *Nat. Microbiol.* **8**, 2183–2195 (2023).
1062 61. Aldridge, K. E. *et al.* Multicenter survey of the changing in vitro antimicrobial susceptibilities of
1063 clinical isolates of Bacteroides fragilis group, Prevotella, Fusobacterium, Porphyromonas, and
1064 Peptostreptococcus species. *Antimicrob. Agents Chemother.* **45**, 1238–1243 (2001).
1065 62. Alauzet, C. *et al.* Metronidazole resistance in Prevotella spp. and description of a new nim gene in
1066 Prevotella baroniae. *Antimicrob. Agents Chemother.* **54**, 60–64 (2010).
1067 63. Holm, J. B. *et al.* Comparative Metagenome-Assembled Genome Analysis of 'Candidatus
1068 Lachnocurva vaginae', Formerly Known as Bacterial Vaginosis-Associated Bacterium-1 (BVAB1).
1069 *Front. Cell. Infect. Microbiol.* **10**, 117 (2020).
1070 64. Fredricks, D. N., Fiedler, T. L. & Marrazzo, J. M. Molecular Identification of Bacteria Associated with
1071 Bacterial Vaginosis. *N. Engl. J. Med.* **353**, 1899–1911 (2005).
1072 65. Vodstrcil, L. A. *et al.* Male-Partner Treatment to Prevent Recurrence of Bacterial Vaginosis. *N.*

1073 *Engl. J. Med.* **392**, 947–957 (2025).
1074 66. Zenilman, J. M. *et al.* Condom Use to Prevent Incident STDs: The Validity of Self-Reported
1075 Condom Use. *Sex. Transm. Dis.* **22**, 15 (1995).
1076 67. Schroder, K. E. E., Carey, M. P. & Vanable, P. A. Methodological challenges in research on sexual
1077 risk behavior: I. Item content, scaling, and data analytical options. *Ann. Behav. Med.* **26**, 76–103
1078 (2003).
1079 68. Schroder, K. E. E., Carey, M. P. & Vanable, P. A. Methodological challenges in research on sexual
1080 risk behavior: II. Accuracy of self-reports. *Ann. Behav. Med.* **26**, 104–123 (2003).
1081 69. Jewanraj, J. *et al.* The Impact of Semen Exposure on the Immune and Microbial Environments of
1082 the Female Genital Tract. *Front. Reprod. Health* **2**, 566559 (2020).
1083 70. Anahtar, M. N., Bowman, B. A. & Kwon, D. S. Efficient Nucleic Acid Extraction and 16S rRNA Gene
1084 Sequencing for Bacterial Community Characterization. *J. Vis. Exp. JoVE* 53939 (2016)
1085 doi:10.3791/53939.
1086 71. Caporaso, J. G. *et al.* Global patterns of 16S rRNA diversity at a depth of millions of sequences per
1087 sample. *Proc. Natl. Acad. Sci. U. S. A.* **108 Suppl 1**, 4516–4522 (2011).
1088 72. Baym, M. *et al.* Inexpensive multiplexed library preparation for megabase-sized genomes. *PloS*
1089 *One* **10**, e0128036 (2015).
1090 73. Caporaso, J. G. *et al.* QIIME allows analysis of high-throughput community sequencing data. *Nat.*
1091 *Methods* **7**, 335–336 (2010).
1092 74. Callahan, B. J. *et al.* DADA2: High-resolution sample inference from Illumina amplicon data. *Nat.*
1093 *Methods* **13**, 581–583 (2016).
1094 75. McMurdie, P. J. & Holmes, S. phyloseq: an R package for reproducible interactive analysis and
1095 graphics of microbiome census data. *PloS One* **8**, e61217 (2013).
1096 76. Aragon, T. J. epitools: Epidemiology Tools. 0.5-10.1
1097 https://doi.org/10.32614/CRAN.package.epitools (2004).

1098 77. Fukuyama, J., Sankaran, K. & Symul, L. Multiscale analysis of count data through topic alignment.
1099 *Biostatistics* **24**, 1045–1065 (2023).
1100 78. Wick, R. R. *et al.* Trycycler: consensus long-read assemblies for bacterial genomes. *Genome Biol.*
1101 **22**, 266 (2021).
1102 79. Bushnell, B. BBMap: A Fast, Accurate, Splice-Aware Aligner. in *Report Number: LBNL-7065E*
1103 (Research Org.: Lawrence Berkeley National Lab. (LBNL), Berkeley, CA (United States), 2014).
1104 80. Kolmogorov, M., Yuan, J., Lin, Y. & Pevzner, P. A. Assembly of long, error-prone reads using
1105 repeat graphs. *Nat. Biotechnol.* **37**, 540–546 (2019).
1106 81. Wick, R. R. & Holt, K. E. Benchmarking of long-read assemblers for prokaryote whole genome
1107 sequencing. *F1000Research* **8**, 2138 (2021).
1108 82. Vaser, R. & Šikić, M. Time- and memory-efficient genome assembly with Raven. *Nat. Comput. Sci.*
1109 **1**, 332–336 (2021).
1110 83. Koren, S. *et al.* Canu: scalable and accurate long-read assembly via adaptive *k* -mer weighting and
1111 repeat separation. *Genome Res.* **27**, 722–736 (2017).
1112 84. Wick, R. R. & Holt, K. E. Polypolish: Short-read polishing of long-read bacterial genome
1113 assemblies. *PLOS Comput. Biol.* **18**, e1009802 (2022).
1114 85. Schwengers, O. *et al.* Bakta: rapid and standardized annotation of bacterial genomes via
1115 alignment-free sequence identification: Find out more about Bakta, the motivation, challenges and
1116 applications, here. *Microb. Genomics* **7**, (2021).
1117 86. Shi, Z. J., Nayfach, S. & Pollard, K. S. Maast: genotyping thousands of microbial strains efficiently.
1118 *Genome Biol.* **24**, 186 (2023).
1119 87. Shi, Z. J., Dimitrov, B., Zhao, C., Nayfach, S. & Pollard, K. S. Fast and accurate metagenotyping of
1120 the human gut microbiome with GT-Pro. *Nat. Biotechnol.* **40**, 507–516 (2022).
1121 88. Martin, M. Cutadapt removes adapter sequences from high-throughput sequencing reads.
1122 *EMBnet.journal* **17**, 10 (2011).

1123 89. Kim, D., Paggi, J. M., Park, C., Bennett, C. & Salzberg, S. L. Graph-based genome alignment and
1124 genotyping with HISAT2 and HISAT-genotype. *Nat. Biotechnol.* **37**, 907–915 (2019).
1125 90. Chaumeil, P.-A., Mussig, A. J., Hugenholtz, P. & Parks, D. H. GTDB-Tk v2: memory friendly
1126 classification with the genome taxonomy database. *Bioinformatics* **38**, 5315–5316 (2022).
1127 91. Hyatt, D. *et al.* Prodigal: prokaryotic gene recognition and translation initiation site identification.
1128 *BMC Bioinformatics* **11**, 119 (2010).
1129 92. Eddy, S. R. HMMER. (2023).
1130 93. Katoh, K., Rozewicki, J. & Yamada, K. D. MAFFT online service: multiple sequence alignment,
1131 interactive sequence choice and visualization. *Brief. Bioinform.* **20**, 1160–1166 (2019).
1132 94. Kuraku, S., Zmasek, C. M., Nishimura, O. & Katoh, K. aLeaves facilitates on-demand exploration of
1133 metazoan gene family trees on MAFFT sequence alignment server with enhanced interactivity.
1134 *Nucleic Acids Res.* **41**, W22–W28 (2013).
1135 95. Price, M. N., Dehal, P. S. & Arkin, A. P. FastTree 2 – Approximately Maximum-Likelihood Trees for
1136 Large Alignments. *PLoS ONE* **5**, e9490 (2010).
1137 96. Price, M. N., Dehal, P. S. & Arkin, A. P. FastTree: Computing Large Minimum Evolution Trees with
1138 Profiles instead of a Distance Matrix. *Mol. Biol. Evol.* **26**, 1641–1650 (2009).
1139 97. Dray, S. & Dufour, A.-B. The **ade4** Package: Implementing the Duality Diagram for Ecologists. *J.*
1140 *Stat. Softw.* **22**, (2007).
1141 98. Bougeard, S. & Dray, S. Supervised Multiblock Analysis in *R* with the **ade4** Package. *J. Stat. Softw.*
1142 **86**, (2018).
1143 99. Abdi, H., Williams, L. J., Valentin, D. & Bennani-Dosse, M. STATIS and DISTATIS: optimum
1144 multitable principal component analysis and three way metric multidimensional scaling. *WIREs*
1145 *Comput. Stat.* **4**, 124–167 (2012).
1146 100. Benjamini, Y. & Hochberg, Y. Controlling the False Discovery Rate: A Practical and Powerful
1147 Approach to Multiple Testing. *J. R. Stat. Soc. Ser. B Methodol.* **57**, 289–300 (1995).

1148 101. Brandolini-Bunlon, M. *et al.* Multi-block PLS discriminant analysis for the joint analysis of
1149 metabolomic and epidemiological data. *Metabolomics* **15**, 134 (2019).
1150 102. Bougeard, S., Qannari, E. M. & Rose, N. Multiblock redundancy analysis: interpretation tools
1151 and application in epidemiology. *J. Chemom.* **25**, 467–475 (2011).
1152

1153 **Main Tables and Figures**

1154 **Table 1: Benefit ratios for LBP microbiota effects**

| Taxon | Week | Microbiota Endpoint | LACTIN-V | Placebo | Benefit Ratio (95% CI) | P Value |
|---|---|---|---|---|---|---|
| *L. crispatus* | Week 12 | ≥ 50% *L.c.* | 37 (30%) | 5 (9%) | 3.37 (1.40 - 8.11) | < 0.005 |
| | | < 50% *L.c.* | 86 (70%) | 51 (91%) | | |
| | Week 24 | ≥ 50% *L.c.* | 39 (35%) | 4 (8%) | 4.49 (1.69 - 11.90) | |
| | | < 50% *L.c.* | 74 (65%) | 48 (92%) | | |
| *Lactobacillus* | Week 12 | ≥ 50% *Lacto* | 69 (56%) | 27 (48%) | 1.16 (0.85 - 1.59) | |
| | | < 50% *Lacto* | 54 (44%) | 29 (52%) | | |
| | Week 24 | ≥ 50% *Lacto* | 65 (58%) | 17 (33%) | 1.76 (1.15 - 2.68) | |
| | | < 50% *Lacto* | 48 (42%) | 35 (67%) | | |

1155 Benefit Ratios and associated 95% confidence intervals were computed using Wald's method.

**Figure 1: LACTIN-V trial design and microbiota endpoints**

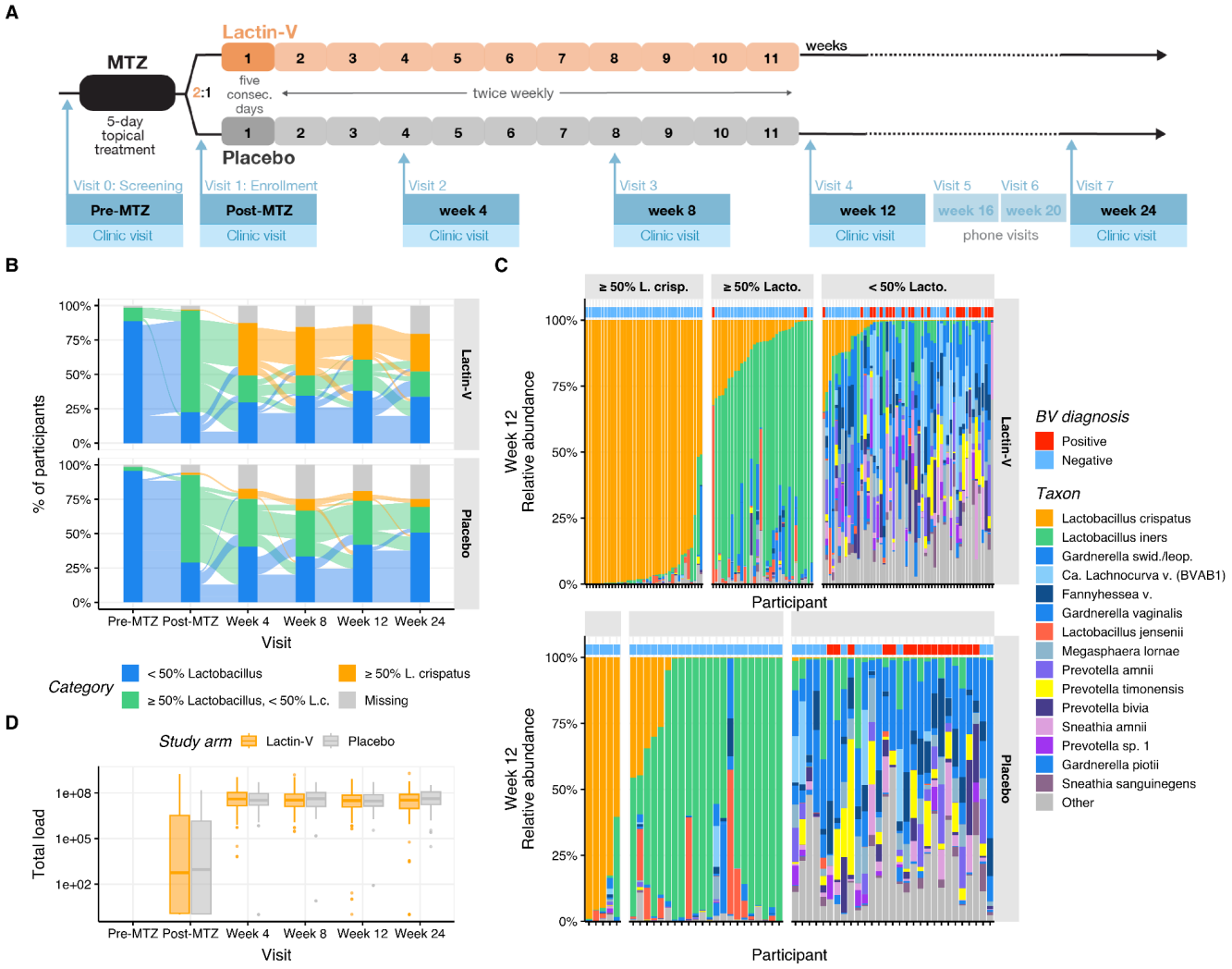


A. Schematic of LACTIN-V trial study design and sampling visit timing.

B. Participants were grouped into three microbiota categories: *L. crispatus*-dominant colonization (≥ 50% *L. crispatus* relative abundance), *Lactobacillus* (non-*crispatus*)-dominant colonization (≥ 50% *Lactobacillus,* < 50% *L. crispatus*), or non-*Lactobacillus*-dominant (< 50% *Lactobacillus*) based on results of bacterial 16S rRNA gene sequencing. The Sankey diagram displays how participants transitioned between these three categories throughout the trial.

1164 C. Microbiota composition and BV diagnosis at week 12 for each participant in the LBP and placebo
1165 treatment arms. Relative abundances of the 15 most abundant taxa are shown, with remaining
1166 taxa summed as “Other”. Participants are grouped by treatment arm into the categories defined
1167 as in **Figure 1B,** with BV diagnosis indicated along the top margin.
1168 D. Total bacterial load (measured by qPCR) at each scheduled visit in each arm. Boxplots (here and
1169 in subsequent figures) represent the median (middle horizontal line), the 25th and 75th percentiles
1170 (lower and upper boundaries of boxes, respectively, “IQR”), measurements that fall within 1.5
1171 times the IQR (whiskers), and any individual measurement outside that range (dots).

1172 **Figure 2: Microbiota trajectories throughout the trial**

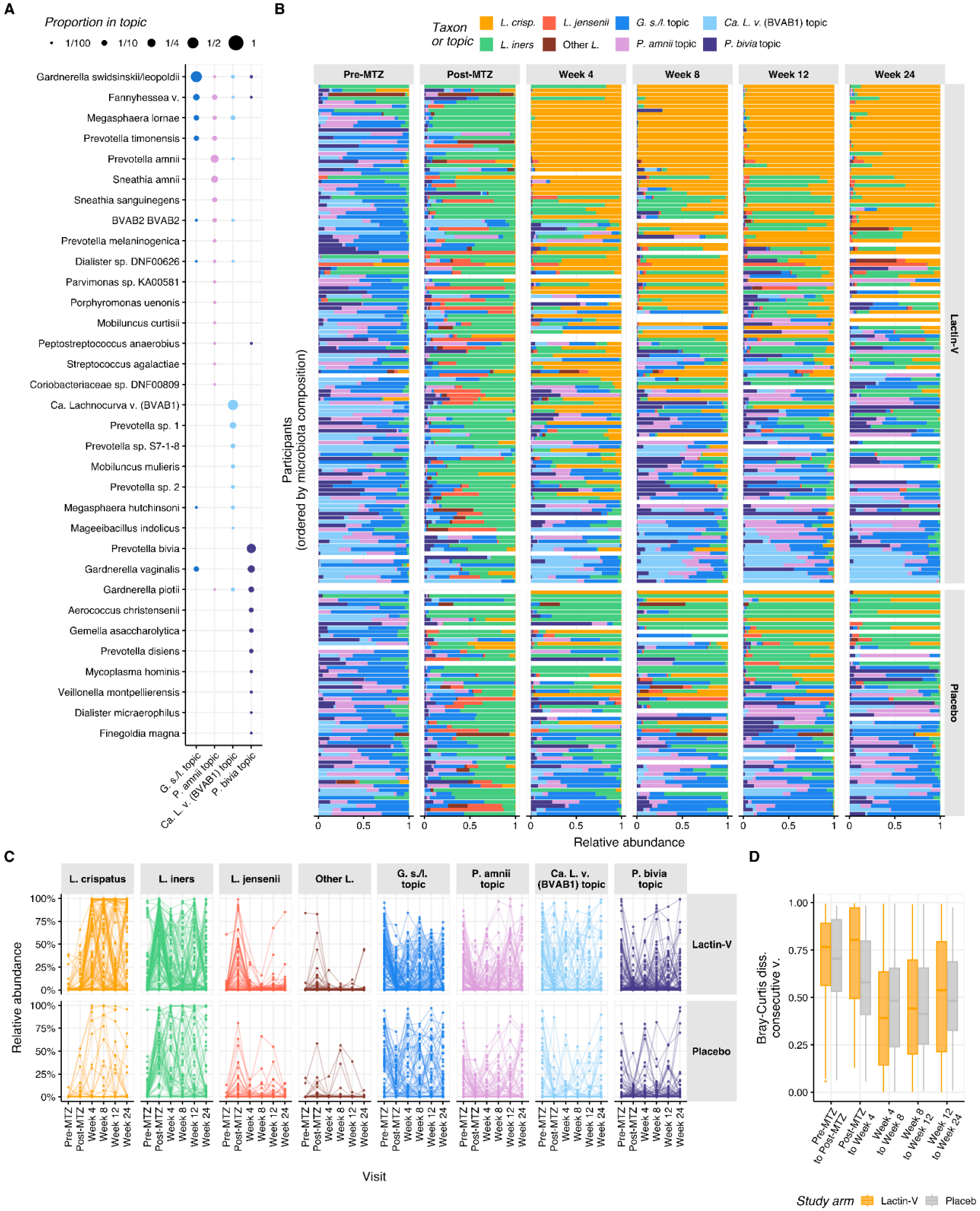
A
Proportion in topic
1/100
1/10
1/4
1/2
1
Gardnerella swidsinskii/leopoldii
Fannyhessea v.
Megasphaera lornae
Prevotella timonensis
Prevotella amnii
Sneathia amnii
Sneathia sanguinegens
BVAB2 BVAB2
Prevotella melaninogenica
Dialister sp. DNF00626
Parvimonas sp. KA00581
Porphyromonas uenonis
Mobiluncus curtisii
Peptostreptococcus anaerobius
Streptococcus agalactiae
Coriobacteriaceae sp. DNF00809
Ca. Lachnocurva v. (BVAB1)
Prevotella sp. 1
Prevotella sp. S7-1-8
Mobiluncus mulieris
Prevotella sp. 2
Megasphaera hutchinsoni
Mageeibacillus indolicus
Prevotella bivia
Gardnerella vaginalis
Gardnerella piotii
Aerococcus christensenii
Gemella asaccharolytica
Prevotella disiens
Mycoplasma hominis
Veillonella montpellierensis
Dialister micraerophilus
Finegoldia magna
G. s./l. topic
P. amnii topic
Ca. L. v. (BVAB1) topic
P. bivia topic
B
Taxon or topic
L. crisp.
L. jensenii
G. s./l. topic
Ca. L. v. (BVAB1) topic
L. iners
Other L.
P. amnii topic
P. bivia topic
Pre-MTZ
Post-MTZ
Week 4
Week 8
Week 12
Week 24
Lactin-V
Placebo
Participants
(ordered by microbiota composition)
0
0.5
1
Relative abundance
C
L. crispatus
L. iners
L. jensenii
Other L.
G. s./l. topic
P. amnii topic
Ca. L. v. (BVAB1) topic
P. bivia topic
Lactin-V
Placebo
Relative abundance
100%
75%
50%
25%
0%
Pre-MTZ
Post-MTZ
Week 4
Week 8
Week 12
Week 24
Visit
D
Bray-Curtis diss. consecutive v.
1.00
0.75
0.50
0.25
0.00
Pre-MTZ to Post-MTZ
Post-MTZ to Week 4
Week 4 to Week 8
Week 8 to Week 12
Week 12 to Week 24
Study arm
Lactin-V
Placeb

1173

1174 A. Proportion of each taxon (y-axis) in each non-*Lactobacillus* topic (x-axis) as estimated by Latent
1175 Dirichlet Allocation (LDA) from 16S rRNA gene sequencing data. Proportions sum to one for each
1176 topic. Taxa were included if they made up at least 1% of any topic and non-*Lactobacillus* topics
1177 are named according to their most predominant taxon. "*G. s/l*": *Gardnerella swidsinskii-leopoldii*.
1178 "*P. amnii*": *Prevotella amnii*. "*Ca.* L. v. (BVAB1)": *Candidatus* Lachnocurva vaginae (BVAB1). "*P.*
1179 *bivia*": *Prevotella bivia*.
1180 B. Microbiota composition expressed as topic relative abundance (x-axis) for each participant at
1181 each scheduled visit. Results are depicted for participants with microbiota compositional data for
1182 at least three of the six visits. Results are grouped by visit (horizontal panels) and treatment arm
1183 (vertical panels), and the y-axis is ordered by microbiota composition trajectories (see **SI**).
1184 C. Relative abundance of each topic (horizontal panels) in each arm (vertical panels) at each visit.
1185 Samples from the same participant are connected by a line.
1186 D. Bray-Curtis dissimilarity between each participant's microbiota composition at the two indicated
1187 consecutive visits, calculated from 16S rRNA gene amplicon sequence variant (ASV) relative
1188 abundances. For each pair of consecutive visits, values are shown only for participants with
1189 available microbiota data from both visits.

1190 **Figure 3: *L. crispatus* strain dynamics among LBP recipients**

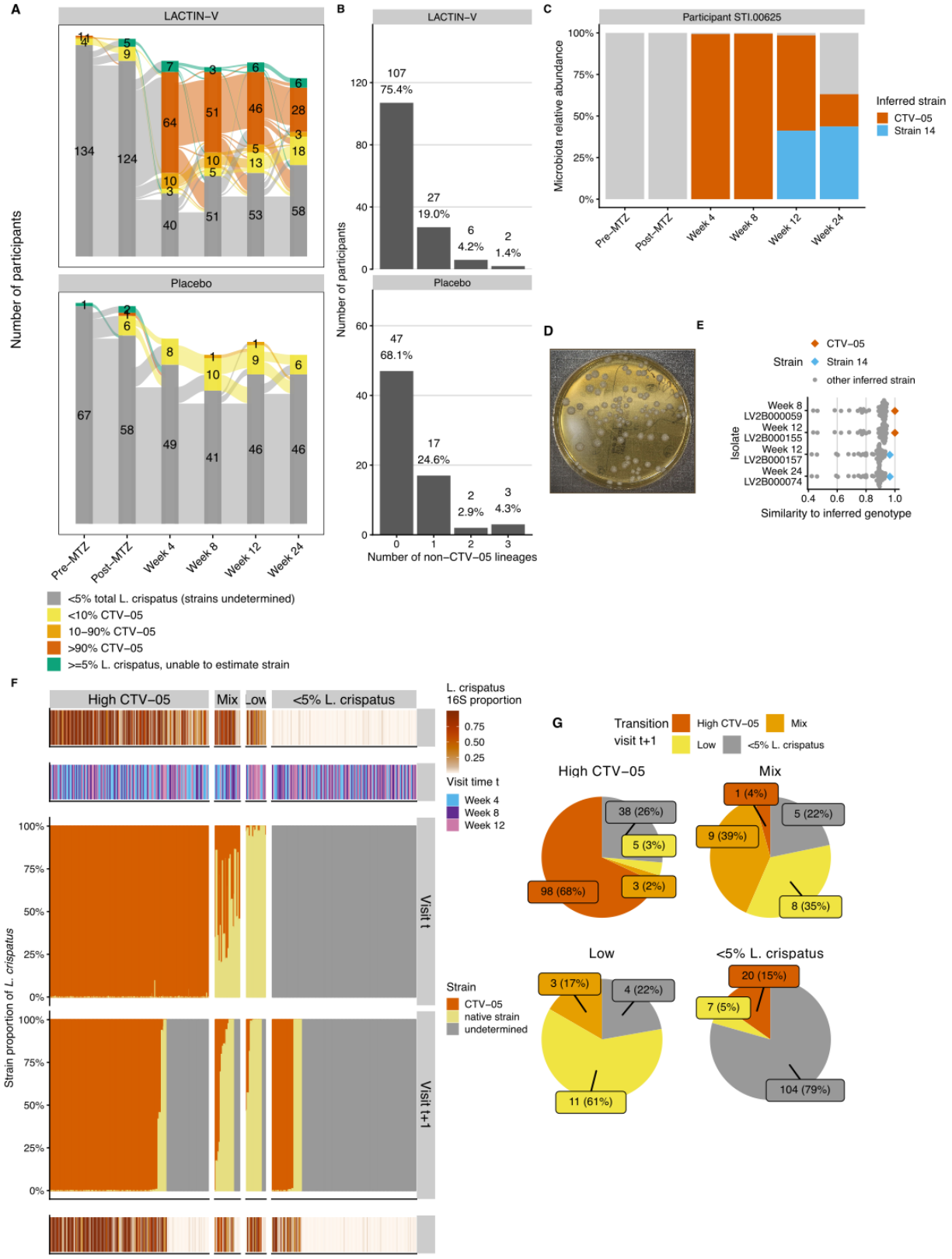
A
LACTIN–V
Placebo
Number of participants
Pre–MTZ
Post–MTZ
Week 4
Week 8
Week 12
Week 24
<5% total L. crispatus (strains undetermined)
<10% CTV–05
10–90% CTV–05
>90% CTV–05
>=5% L. crispatus, unable to estimate strain
B
LACTIN–V
Placebo
Number of participants
107
75.4%
27
19.0%
6
4.2%
2
1.4%
47
68.1%
17
24.6%
2
2.9%
3
4.3%
Number of non–CTV–05 lineages
C
Participant STI.00625
Microbiota relative abundance
Inferred strain
CTV–05
Strain 14
D
E
Strain
CTV–05
Strain 14
other inferred strain
Isolate
Week 8
LV2B000059
Week 12
LV2B000155
Week 12
LV2B000157
Week 24
LV2B000074
Similarity to inferred genotype
F
High CTV–05
Mix
Low
<5% L. crispatus
L. crispatus
16S proportion
Visit time t
Week 4
Week 8
Week 12
Strain proportion of L. crispatus
Visit t
Visit t+1
Strain
CTV–05
native strain
undetermined
G
Transition
visit t+1
High CTV–05
Mix
Low
<5% L. crispatus
High CTV–05
38 (26%)
5 (3%)
3 (2%)
98 (68%)
Mix
1 (4%)
5 (22%)
9 (39%)
8 (35%)
Low
3 (17%)
4 (22%)
11 (61%)
<5% L. crispatus
20 (15%)
7 (5%)
104 (79%)

1191

1192 A. Sankey diagram showing dynamics of CTV-05 versus non-CTV-05 *L. crispatus* strain colonization
1193 among LBP recipients. Strains were inferred from shotgun metagenomic whole genome
1194 sequencing (mWGS) using StrainFacts for all samples with ≥5% total *L. crispatus* relative
1195 abundance as determined from 16S rRNA gene sequencing. Samples were categorized based
1196 on proportional *L. crispatus* strain abundance as >90% CTV-05 ("High CTV-05"), 10-90% CTV-
1197 05 ("Mixed"), <10% CTV-05 ("Low CTV-05"). Strain inference was unsuccessful for a small
1198 fraction of samples (depicted in green) due to technical failures of metagenomic sequencing.
1199 B. Histograms showing the number (percentage) of study participants in each treatment arm with
1200 the indicated number of inferred native (non-CTV-05) *L. crispatus* strains detected at least once
1201 during the trial.
1202 C. Metagenomically inferred *L. crispatus* strain composition throughout the trial in an example
1203 participant from whom targeted isolations were performed at weeks 8, 12, and 24. The plot depicts
1204 overall microbiota relative abundance, with non-*L. crispatus* species summed (gray) and inferred
1205 *L. crispatus* strains shown individually in red (CTV-05 strain) and blue (a native strain: "Strain 14").
1206 D. Example *Lactobacillus* MRS agar plate from bacterial isolations showing characteristic *L.*
1207 *crispatus* colony morphology.
1208 E. Genomes of *L. crispatus* isolated from the week 8, 12, and 24 visits of the participant in **Figure**
1209 **3C** identified two strains nearly identical to the metagenomically inferred strains in these samples
1210 (assessed by Jaccard similarity to StrainFacts-inferred genotypes) and dissimilar from all other
1211 inferred strains in the cohort, none of which were detected in this participant's samples. The
1212 isolated strains included the CTV-05 strain isolated from week 8 and 12 samples (red), and native
1213 Strain 14 isolated from week 12 and 24 samples (blue; see also **Figure S3A**).
1214 F. Transition plot for LBP recipients showing total *L. crispatus* relative abundance (determined by
1215 16S rRNA gene sequencing, top and bottom rows) and strain category proportions (third and

1216 fourth rows) at each pair of consecutively scheduled post-randomization visits with available strain
1217 inference data or at which strain inference was not performed due to <5% total *L. crispatus* relative
1218 abundance. Strain categories in the third and fourth rows show proportions of observed *L.*
1219 *crispatus* representing CTV-05 versus the sum of the native strain(s) at each visit; "undetermined"
1220 refers to samples in which strain inference was not performed. Pairs including a visit in which
1221 strain inference was unsuccessful due to technical failures of metagenomic sequencing are not
1222 shown. For each pair of visits, the top three panels show *L. crispatus* relative abundance, visit
1223 week, and strain category at the first visit in the pair ("Visit t") and the bottom two panels show
1224 strain category and relative abundance at the subsequent visit ("Visit t+1"). Visit pairs are grouped
1225 along the horizontal axis by strain category at Visit t and ordered within groups by CTV-05 strain
1226 proportion at Visit t+1.

1227 G. Pie charts for each Visit t strain category from **Figure 3F**, summarizing subsequent *L. crispatus*
1228 strain category frequencies at Visit t+1.

1229 **Figure 4: Treatment effects on mucosal inflammation and relationship to microbiota composition.**

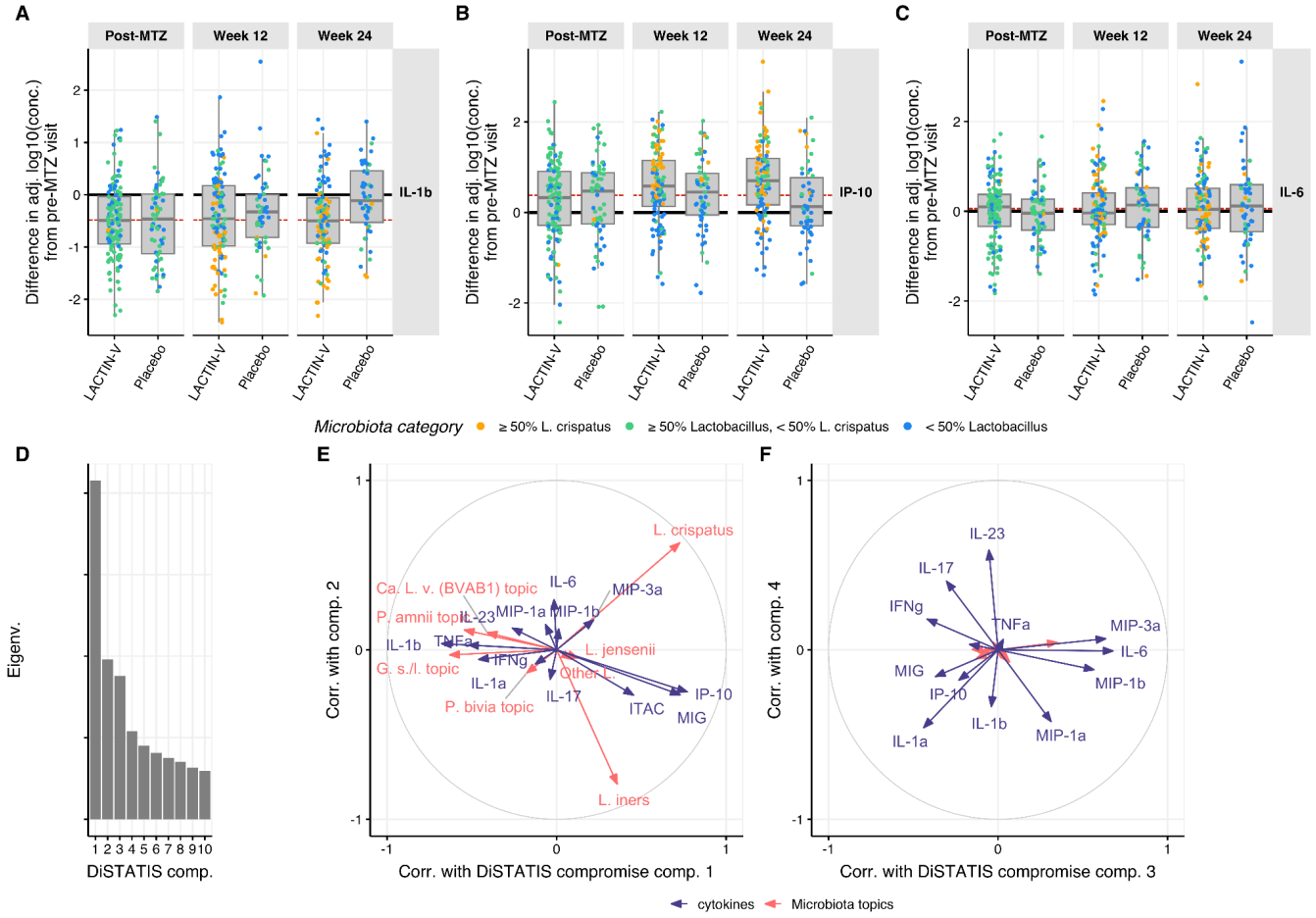


1230

1231 A. Differences in log10-transformed, adjusted IL-1β concentrations between participants' pre-MTZ
1232 visit and their ensuing post-MTZ, week 12, and week 24 visits (horizontal panels) in both treatment
1233 arms. Each dot represents a single visit per participant.

1234 B. Same as **Figure 4A**. for IP-10 adjusted concentrations.

1235 C. Same as **Figure 4A**. and **4B** for IL-6 adjusted concentrations. Similar displays are available for
1236 all cytokine adjusted concentrations and non-adjusted concentrations in the **SI**.

1237 D. DiSTATIS screeplot: eigenvalues (a.u.) of DiSTATIS compromise for the first 10 latent
1238 components.

1239 E. DiSTATIS correlation circle showing the correlations between the 1st (x-axis) and 2nd (y-axis)
1240 DiSTATIS compromise latent dimension and the microbiota topic proportions (red) or cytokine
1241 transformed concentrations (blue).
1242 F. Same as **Figure 4E** for DiSTATIS 3rd and 4th latent components.

1243 **Figure 5: Heterogeneity in intervention effects with respect to pre-MTZ microbiota**

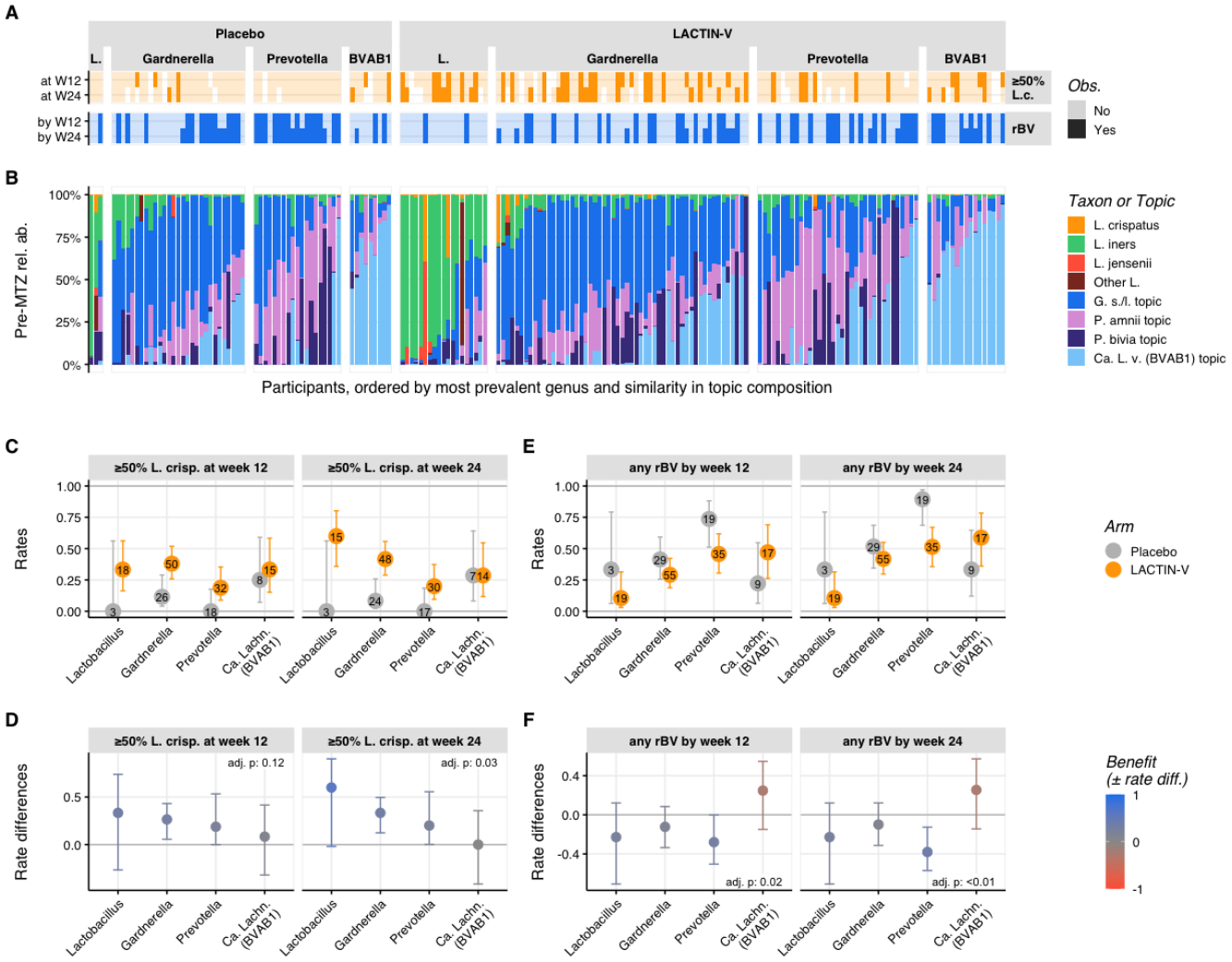


1244

1245 A. Participant-level observed outcomes for attainment of *L. crispatus*-dominance at weeks 12 and

1246 24 (dark orange: ≥50% *L. crispatus*; light orange <50% *L. crispatus*) and BV recurrence by weeks

1247 12 and 24 (dark blue: rBV; light blue: no rBV) for each participant with week 12 and/or week 24

1248 data. White indicated data not available. Participants are grouped according to treatment arm

1249 and, within treatment arm, by the most predominant bacterial genus at their pre-MTZ visit ("L."

1250 indicates *Lactobacillus*; “BVAB1” indicates *Ca.* Lachnocurva vaginae). Predominant-genus
1251 groupings lacking at least two participants in each treatment arm were excluded.

1252 B. Pre-MTZ microbiota composition for each participant in **Figure 5A** (x-axis ordered and vertically
1253 aligned as in **5A**), expressed as topic proportions (see **Figure 2A** for topic definitions).

1254 C. Rates and associated 95% CI of *L. crispatus*-dominance (≥50% *L. crispatus*) at week 12 or 24
1255 (horizontal panels) by pre-MTZ microbiota group in each arm. Participants are grouped based on
1256 their most predominant genus as defined in **Figure 5A-B**. CI are computed using Wilson's scores
1257 due to low sample sizes in some groups.

1258 D. Rate differences (rate in LBP arm - rate in placebo arm) and associated 95% CI (Wilson’s score
1259 method) between arms for results in **Figure 5C**. Color scale shows degree of benefit (defined as
1260 the difference in rates between the two arms) in achieving *L. crispatus*-dominance, with blue
1261 indicating benefit with LBP treatment and red indicating benefit with placebo. *P*-values adjusted
1262 for multiple testing (across panel **5D** and **5F**) using the Benjamini-Hochberg correction of the
1263 analysis of deviance test for heterogeneity in treatment effects when stratifying participants
1264 according to their most predominant genus at the pre-MTZ visit are shown in upper right corner.

1265 E. Same as (**Figure 5C**), but for BV recurrence by week 12 or 24.

1266 F. Same as (**Figure 5D**), but for BV recurrence by week 12 or 24. Color scale shows degree of
1267 benefit in reducing rBV, with blue indicating benefit with LBP treatment and red indicating benefit
1268 with placebo.

1269 **Figure 6: Multiblock analysis of factors associated with microbiota categories in LACTIN-V**

1270 **recipients.**

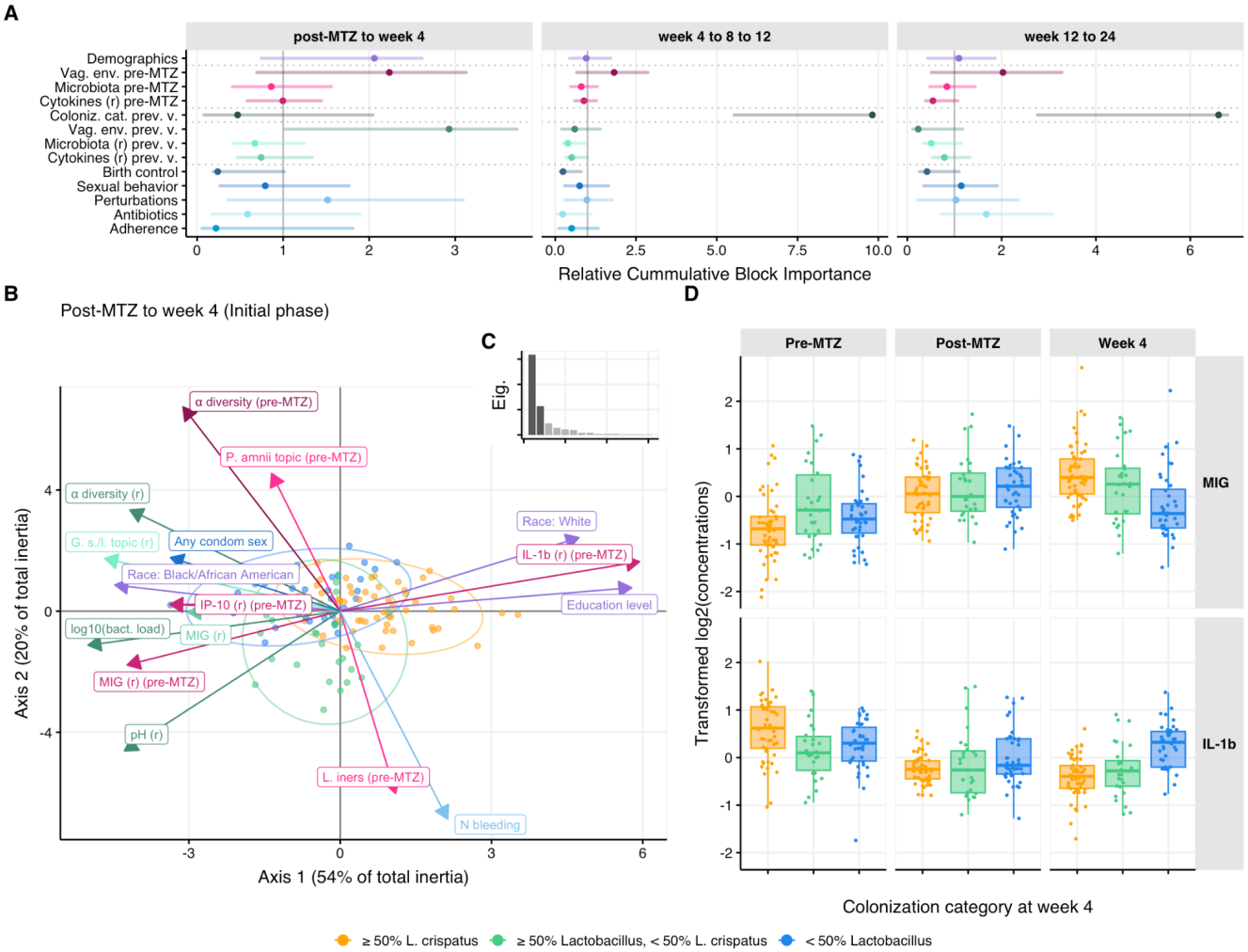


1271

1272 A. Multiblock partial least squared discriminant analysis (MB-PLS-DA, **Figure S6A**) of factors

1273 predictive of microbiota categories (≥50% *L. crispatus*; ≥50% *Lactobacillus* and <50% *L.*

1274 *crispatus*; or <50% *Lactobacillus*) at the indicated visits. Relative cumulative importance indices

1275 (x-axis, Methods) are shown for each thematic block of explanatory variables (y-axis, color) for

1276 the initial phase model (post-MTZ to Week 4; left panel), continuation phase model (Week 4 to 8

1277 to 12; middle panel), and follow-up phase model (Week 12 to 24; right panel). Dots indicate point

1278 estimates and translucent horizontal bars represent bootstrapped 95% CI. Vertical lines at x = 1
1279 show the expected value under the (null) hypothesis that all variables have the same importance.
1280 Block definitions along with the description of the variables included in each block are provided in
1281 **Table S6**. Horizontal dashed lines separate blocks included in the nested models (**Figure S6A**,
1282 **SI**, Methods).

1283 B. Bi-plot for the MB-PLS-DA initial phase model (from post-MTZ to week 4). Dots represent scores
1284 (each dot is a participant) while arrows represent loadings (each arrow is an explanatory variable,
1285 see **Figure S7A**) for the most important variables (Methods) in the space of the 2 first latent
1286 variables. Dots (participants) are colored by their corresponding response categories (*i.e.,* their
1287 colonization status at week 4). Perfect separation of the categories would indicate perfect
1288 prediction of colonization status at the week 4 visit. Arrows (explanatory variables) are colored by
1289 the block to which they belong to - **Figure 6A** and **Table S6** serve as color legend.

1290 C. Scree-plot of the first 15 eigenvalues of the model from **Figure 6B**. The first two latent variables
1291 (selected by cross-validation) are shown in dark gray.

1292 D. Transformed $\log_2$-concentrations (y-axis) of two cytokines (MIG and IL-1b) whose pre-MTZ levels
1293 (left panel) were identified as associated with participants' colonization status at week 4 (x-axis,
1294 colors) by the model (**Figure 6A** and **S7A**). Concentrations at the post-MTZ and week 4 visits are
1295 shown in the middle and right panels. Each dot is a participant, colored by the colonization status
1296 at week 4 for each panel.

1297 **Supplementary Tables and Figures**

1298 **Table S1**

| | At least one visit | Pre-MTZ | Post-MTZ | Week 4 | Week 8 | Week 12 | Week 24 | All planned in-person visits |
|---|---|---|---|---|---|---|---|---|
| **Total** | 211 | 208 | 203 | 181 | 172 | 179 | 165 | 139 |
| **LACTIN-V** | 142 | 140 | 138 | 124 | 120 | 123 | 113 | 99 |
| **Placebo** | 69 | 68 | 65 | 57 | 52 | 56 | 52 | 40 |

1299 Number of participants in each study arm (rows) with available 16S rRNA gene sequencing data at any,

1300 each, or all planned in-person visits (unscheduled clinic visits not shown).

1301 **Table S2**

| | % (n) [both arm] | % (n) [LACTIN-V] | % (n) [Placebo] |
|---|---|---|---|
| ≥ 50% *L. iners* | 52 % (106) | 52 % (72) | 52 % (34) |
| ≥ 50% *L. jensenii* | 8 % (16) | 9 % (13) | 5 % (3) |
| ≥ 50% *L. crispatus* | 1 % (2) | 1 % (1) | 2 % (1) |
| ≥ 50% *Lactobacillus* (no individual species ≥ 50%) | 13 % (27) | 14 % (20) | 11 % (7) |
| < 50% *Lactobacillus* | 26 % (52) | 23 % (32) | 31 % (20) |

1302 At the post-MTZ visit, number and proportion of samples dominated by one of the top *Lactobacillus*
1303 species (top 3 rows), a mixture of *Lactobacillus* (4th row), or by non-*Lactobacillus* species in both arms
1304 (2nd column), the LACTIN-V arm (3rd column), or the placebo arm (4th column).

1305 **Table S3**

| | Clinical diagnosis | |
|---|---|---|
| **Microbiota outcome** (16S rRNA sequencing-based) | no rBV n (%) | rBV n (%) |
| < 50% *Lactobacillus* | 162 (50 %) | 164 (50 %) |
| ≥ 50% *Lactobacillus, <50% L. crispatus* | 192 (99 %) | 2 (1 %) |
| ≥ 50% *L. crispatus* | 209 (100 %) | 0 (0 %) |

1310 Number of visits (n) at which

1311 participants did not (left column) or did (right column) meet diagnostic criteria for recurrent BV (rBV).

1312 Participants are shown according to microbiota category. Percentages sum to 100% for each category.

1313 **Table S4**

| Category at week 4 | Category at **week 12** | | | |
|---|---|---|---|---|
| | ≥ 50% *L. crispatus* | ≥ 50% *Lactobacillus*, < 50% *L. crispatus* | < 50% *Lactobacillus* | Total |
| ≥ 50% *L. crispatus* | 25 | 14 | 12 | 51 |
| ≥ 50% *Lactobacillus*, < 50% *L. crispatus* | 6 | 12 | 8 | 26 |
| < 50% *Lactobacillus* | 4 | 4 | 30 | 38 |
| Total | 35 | 30 | 50 | 115 |

1314 Contingency table showing the correspondence between Week 4 and Week 12 microbiota categories for

1315 LACTIN-V recipients with available data from both visits.

1316 **Table S5**

| Category at week 4 | Category at **week 24** | | | |
|---|---|---|---|---|
| | ≥ 50% *L. crispatus* | ≥ 50% *Lactobacillus*, < 50% *L. crispatus* | < 50% *Lactobacillus* | Total |
| ≥ 50% *L. crispatus* | 27 | 9 | 11 | 47 |
| ≥ 50% *Lactobacillus*, < 50% *L. crispatus* | 6 | 6 | 11 | 23 |
| < 50% *Lactobacillus* | 5 | 10 | 22 | 37 |
| Total | 38 | 25 | 44 | 107 |

1317 Contingency table showing the correspondence between Week 4 and Week 24 microbiota categories for

1318 LACTIN-V recipients with available data from both visits.

1319 **Table S6**

| Block | Variable | Description |
|---|---|---|
| Demographics | Age | Age of the participant at enrollment. |
| | N past BV | Number of past BV episodes (coded as a number on the following scale: (1) None, (2) 1-2, (3) Unknown, (4) 3-4, (5) 5 or more). |
| | Education level | Education level of the participant (coded as a number on the following scale: (1) Did not complete high school, (2) Completed high school, (3) Completed junior college, (4) Completed college (undergraduate degree), (5) Completed graduate degree). |
| | Race | Self-declared race of the participant (Categories with few participants were merged into "Other"). |
| Vag. env. pre-MTZ | α diversity | Shannon diversity index of baseline (pre-MTZ) microbiota, computed on taxa proportions quantified from 16S rRNA gene sequencing data. |
| | pH | Vaginal pH at the pre-MTZ visit, measured at study sites. |
| Microbiota pre-MTZ | | Pre-MTZ microbiota composition described as topic proportions. |
| Cytokine (r) pre-MTZ | | Pre-MTZ cytokine residual levels. These values are computed as the difference between the transformed cytokine/chemokines levels and their predicted value based on microbiota composition expressed as topic proportions. |
| Coloniz. cat. prev. v. | | Colonization category at the previous visit. One of these mutually exclusive categories: ≥ 50% *L. crispatus*, ≥ 50% *Lactobacillus* and < 50% *L. crispatus*, or < 50% *Lactobacillus*. |
| Vag. env. prev. v. | α diversity (r) | Difference between the Shannon diversity index at the previous visit (w.r.t the visit of the response variable), computed on taxa proportions quantified from 16S rRNA gene sequencing data, and its expected value based on colonization category at the same visit. |
| | pH (r) | Difference between vaginal pH at the previous visit, measured at study sites, and its expected value based on colonization category at the same visit. |
| | log10(bact. load) | $Log_{10}$ total bacterial load at the previous visit, quantified by qPCR. |
| Microbiota (r) prev. v. | | Difference between the observed microbiota composition at the previous visit described as topic proportions and the average microbiota composition within each colonization category. |
| Cytokines (r) prev. v. | | Cytokine residual levels at the previous visit. These values are computed as the difference between the transformed cytokine/chemokines levels and their predicted value based on microbiota composition expressed as topic proportions. |
| Birth control | Non-hormonal | A binary variable indicating whether participants reported exclusively using one of the following non-hormonal birth control methods including abstinence, use of condoms, or fertility awareness methods. |
| | IUD (Hormonal) | Same as above for hormonal intra-uterine device. |
| | IUD (Non-hormonal) | Same as above for non-hormonal intra-uterine device (copper IUD). |

| | | |
|---|---|---|
| | Combined | A binary variable indicating whether participants reported using a combination of hormonal contraceptives or switched contraceptive method between the last visit and this one. |
| | P only | A binary variable indicating whether participants reported exclusively using progestin-only hormonal contraceptive, including the pill, patches, and implants. |
| | unknown | A binary variable indicating whether a participant's birth control is unknown (missing data). Each participant belongs to only one of each birth control category. |
| Sexual behavior | N new partners | Number of new sexual partners since the last visit. |
| | Any condomless sex | A binary flag indicating whether the participant reported any sexual intercourse without condoms since the last visit. |
| | Any condom sex | A binary flag indicating whether the participant reported any sexual intercourse with condoms since the last visit. |
| Perturbations | N douching | Number of days participant reported any douching episode since the last visit. |
| | N bleeding | Number of days participant reported vaginal bleeding since the last visit. |
| Antibiotics | N vag. abx | Number of days participant reported using vaginal antibiotics since the previous visit. |
| | N oral abx | Number of days participant reported taking oral antibiotics since the previous visit. |
| Adherence | N missed doses | Difference between the number of LACTIN-V doses that should have been taken between the previous visit and the current visit if the study protocol had been strictly followed and the actual number of doses that were taken. |
| | Days since last dose | Number of days since the most recent LACTIN-V dose was taken. |

1320

**Figure S1**

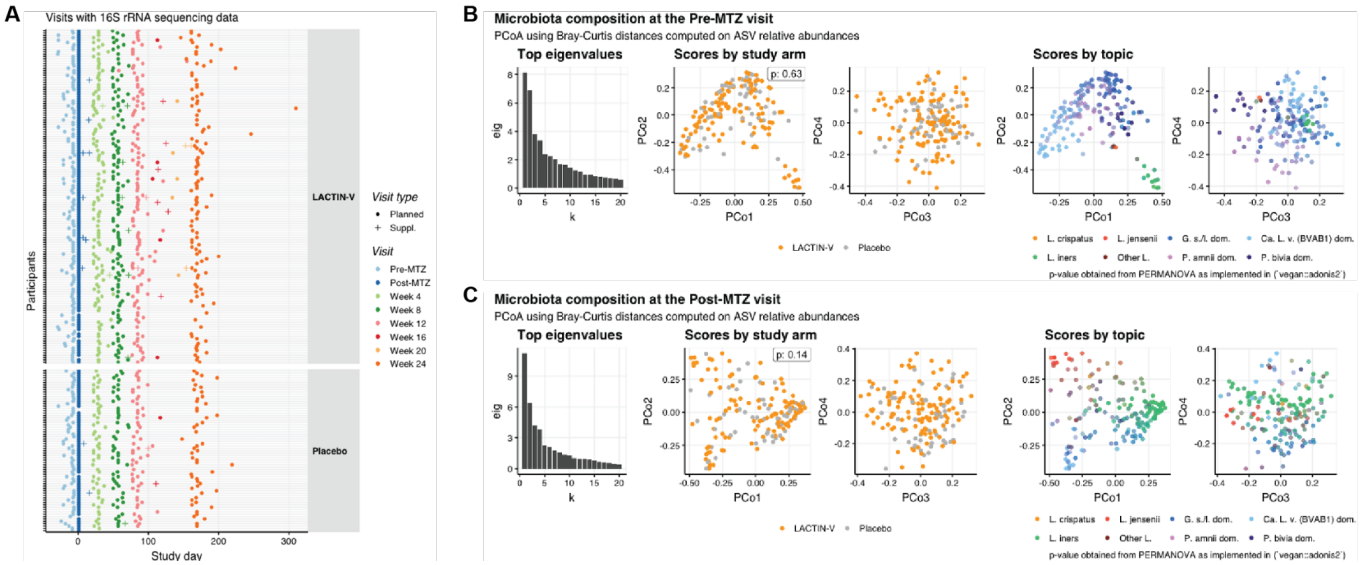


A. Time-line of collected swabs from which 16S rRNA gene sequencing data could be generated.

B. Balance between treatment arms in terms of microbiota composition at the pre-MTZ visit. The left panel shows the top 20 eigenvalues of the PCoA (Principal Coordinate Analysis) performed on the Bray-Curtis dissimilarity matrix, computed from the relative abundances of ASVs. The next two panels show the PCoA scores (projection of the samples, each dot is a sample) colored by the intervention arm for the first 4 principal coordinates. The *p*-value in the upper right corner corresponds to the PERMANOVA test on the study arm. The right panels show the same projections as the middle panels, but samples are here colored by topic relative abundance (**Figure 2A-B**).

C. Balance between treatment arms in terms of microbiota composition at the post-MTZ visit, labeled and arranged as for **Figure S1B**.

1334 **Figure S2**

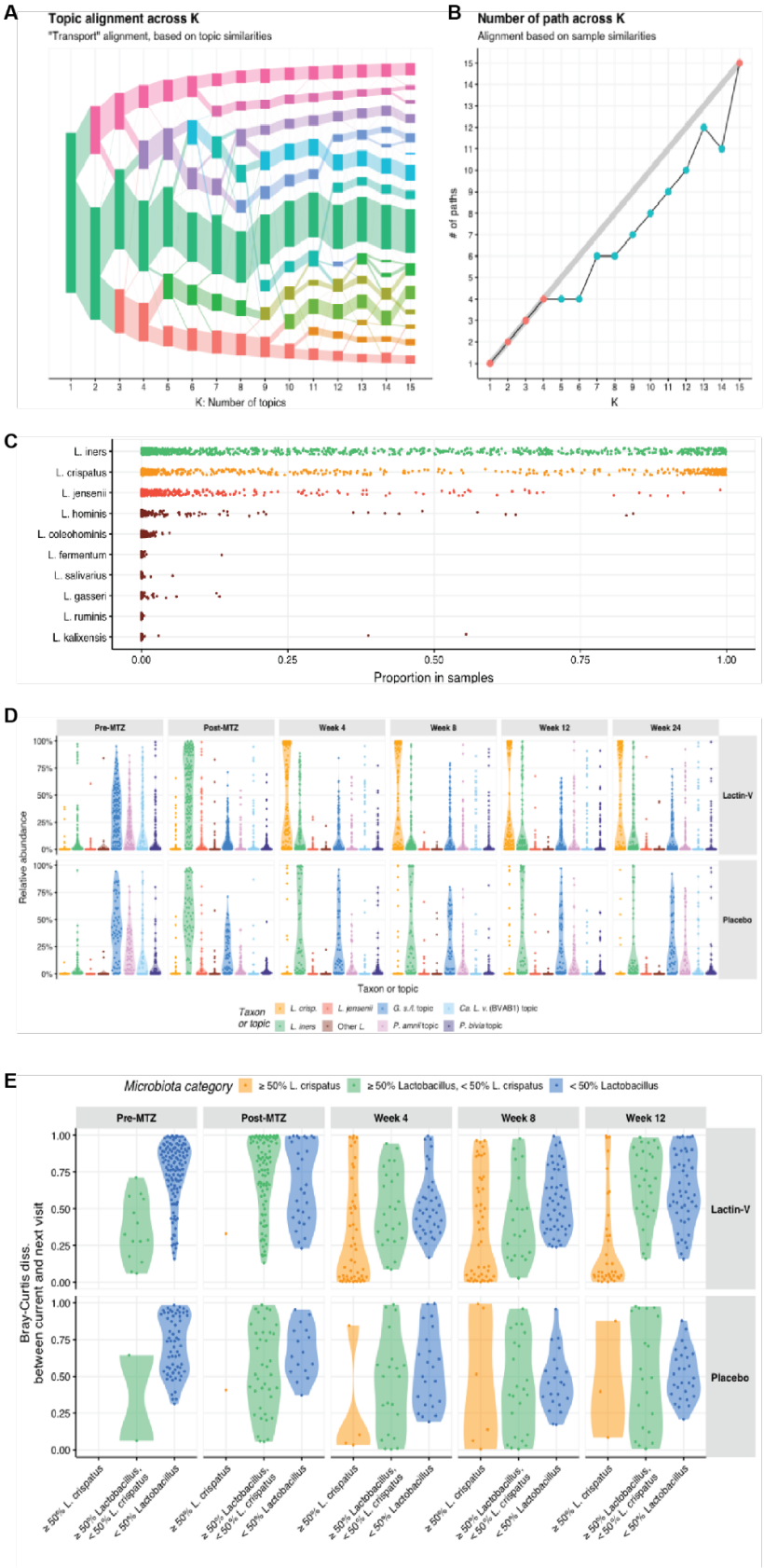
A
Topic alignment across K
"Transport" alignment, based on topic similarities
K: Number of topics
B
Number of path across K
Alignment based on sample similarities
# of paths
K
C
L. iners
L. crispatus
L. jensenii
L. hominis
L. coleohominis
L. fermentum
L. salivarius
L. gasseri
L. ruminis
L. kalixensis
Proportion in samples
D
Pre-MTZ
Post-MTZ
Week 4
Week 8
Week 12
Week 24
Lactin-V
Placebo
Relative abundance
Taxon or topic
Taxon or topic
L. crisp.
L. jensenii
G. a./f. topic
Ca. L. v. (BVAB1) topic
L. iners
Other L.
P. amnii topic
P. bivia topic
E
Microbiota category
≥ 50% L. crispatus
≥ 50% Lactobacillus, < 50% L. crispatus
< 50% Lactobacillus
Pre-MTZ
Post-MTZ
Week 4
Week 8
Week 12
Lactin-V
Placebo
Bray-Curtis diss. between current and next visit

1335

1336 A. “Transport” alignment between topics identified by LDA models fitted on the non-*Lactobacillus*
1337 taxa counts for varying total number of topics (K, x-axis). Each rectangle represents a topic; the
1338 height of that rectangle represents the summed prevalence of that topic in the population, and the
1339 size of the connection between topics is proportional to the degree of similarity between the
1340 composition of two given topics.
1341 B. The number of paths (y-axis) identified at each resolution (K, the number of topics considered by
1342 the LDA models, x-axis) from the “product” alignment of topics; for details see[77]. A path identifies
1343 a series of topics with high alignment scores throughout resolutions. A plateau in the number of
1344 paths (here at K = 4) suggests that the 4-topic model is the model that identifies most robust
1345 topics (i.e., topics that remain similar across resolution despite the introduction of new, potentially
1346 spurious, topics).
1347 C. Proportion (x-axis) of each *Lactobacillus* species (y-axis) detected across all samples. Species
1348 with a relative abundance > 50% in at least 10 samples made up their own topic.
1349 D. Relative abundance of taxon or topic (x-axis, colors) in each arm at each visit.
1350 E. Microbiota stability by arm, visit, and microbiota category. Stability is quantified using the Bray-
1351 Curtis dissimilarity, described as relative abundances at the ASV level at the participant’s current
1352 visit (vertical panels) and subsequent scheduled visit. At each visit, participants are grouped into
1353 one of the three categories (colors, x-axis) defined earlier (*L. crispatus*-dominant, *Lactobacillus*-
1354 dominant but low-level *L. crispatus*, and low-level *Lactobacillus*).

1355 **Figure S3**

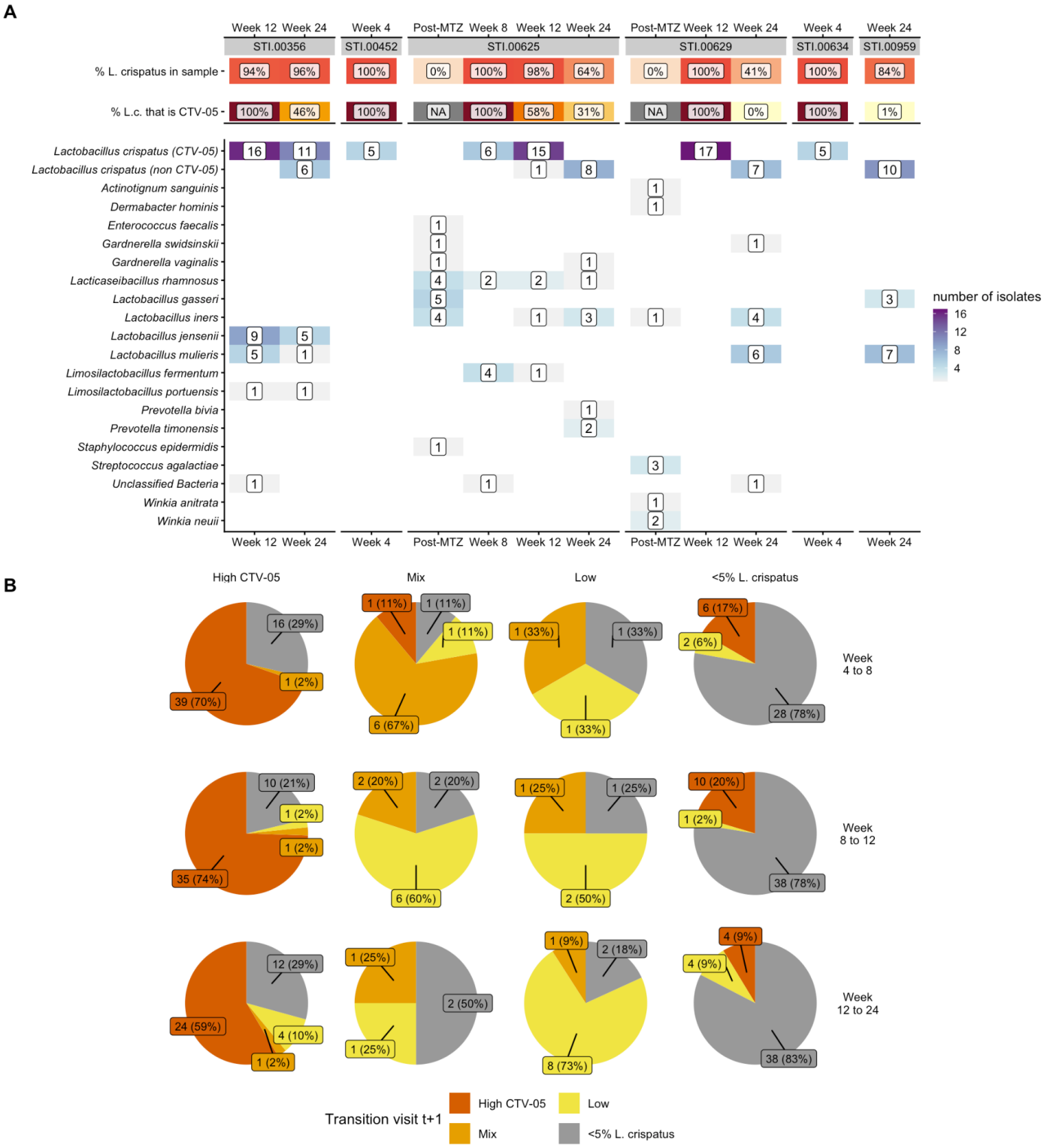


1356

1357 A. Results of targeted isolations from LACTIN-V trial samples, showing source participant, visit
1358 number, sample *L. crispatus* relative abundance as estimated by 16S rRNA gene sequencing,
1359 CTV-05 proportional strain abundance, and the numbers and taxonomic assignments of
1360 genome-sequenced isolates from each sample. *L. crispatus* isolates are separated by whether
1361 genome sequencing showed them to be CTV-05 or non-CTV-05 (native) strains. Multiple
1362 isolates of genotypically identical strains (including of *L. crispatus* isolates) were obtained from
1363 some samples.
1364 B. Pie charts for each Visit t strain category from **Figure 3F** summarizing *L. crispatus* strain category
1365 frequencies at Visit t+1, shown individually for each Visit t.

**Figure S4**

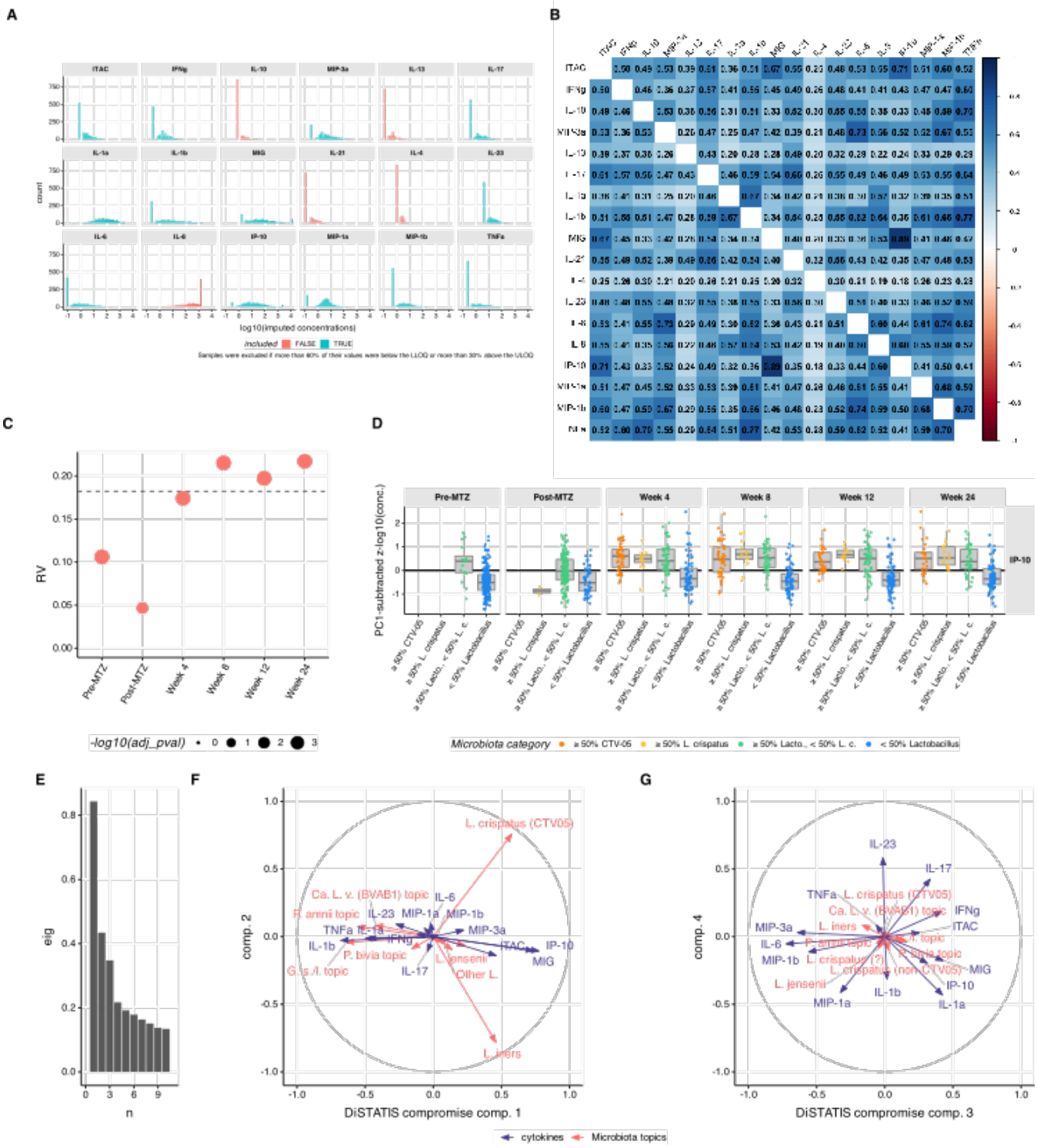


1367

1368 A. Distribution of unadjusted cytokine and chemokine concentrations within the dataset, with values
1369 below the lower limit of quantification (LLOQ) imputed at half the LLOQ and values above the
1370 upper limit of quantification (ULOQ) imputed at the ULOQ. Analytes were excluded from further
1371 analysis if >60% of values were below the LLOQ or >30% were above the ULOQ.
1372 B. Pair-wise Pearson correlation coefficients between log10-transformed concentrations of each
1373 cytokine. All correlations were significant ($p < 0.05$).
1374 C. RV coefficients (y-axis) between microbiota composition described in terms of topic proportions
1375 and cytokine/chemokine transformed concentrations at each visit (x-axis). Permutation test *p*-
1376 values were adjusted for multiple testing to control for the false discovery rate. The size of the dot
1377 is inversely proportional to the $\log_{10}$ of the associated adjusted p-value. The horizontal dashed
1378 line provides the value of the RV coefficient when computed on all visits combined.
1379 D. IP-10 adjusted $\log_{10}$(concentrations) (y-axis) by microbiota composition categories (x-axis) at
1380 each visit (horizontal panels). Microbiota categories are mutually exclusive such that the first
1381 category (≥ 50% CTV-05) encompasses samples in which the relative abundance of CTV-05
1382 (within the overall microbiota) is larger or equal to 50%; the second category encompasses
1383 samples with ≥50% total *L. crispatus* but <50% CTV-05 relative abundance within the microbiota;
1384 the third category includes samples in which total *L. crispatus* relative abundance is <50%, but
1385 the total *Lactobacillus* relative abundance is ≥50%, and the remaining category includes samples
1386 with <50% *Lactobacillus*. Participants from both arms are included.
1387 E. DISTATIS screeplot from repeated DiSTATIS analysis, similar to analysis in **Figure 4D** but
1388 differentiating between CTV-05 and summed other *L. crispatus* strains. Eigenvalues (a.u.) of
1389 DISTATIS compromise for the first 10 latent components are shown.

1390 F. DISTATIS correlation circle for the analysis in **Figure S4E**, showing the 1st and 2nd latent
1391 components (similar to **Figure 4E**).
1392 G. DISTATIS correlation circle for the analysis in **Figure S4E**, showing the 3rd and 4th latent
1393 components (similar to **Figure 4F**).

1394 **Figure S5**

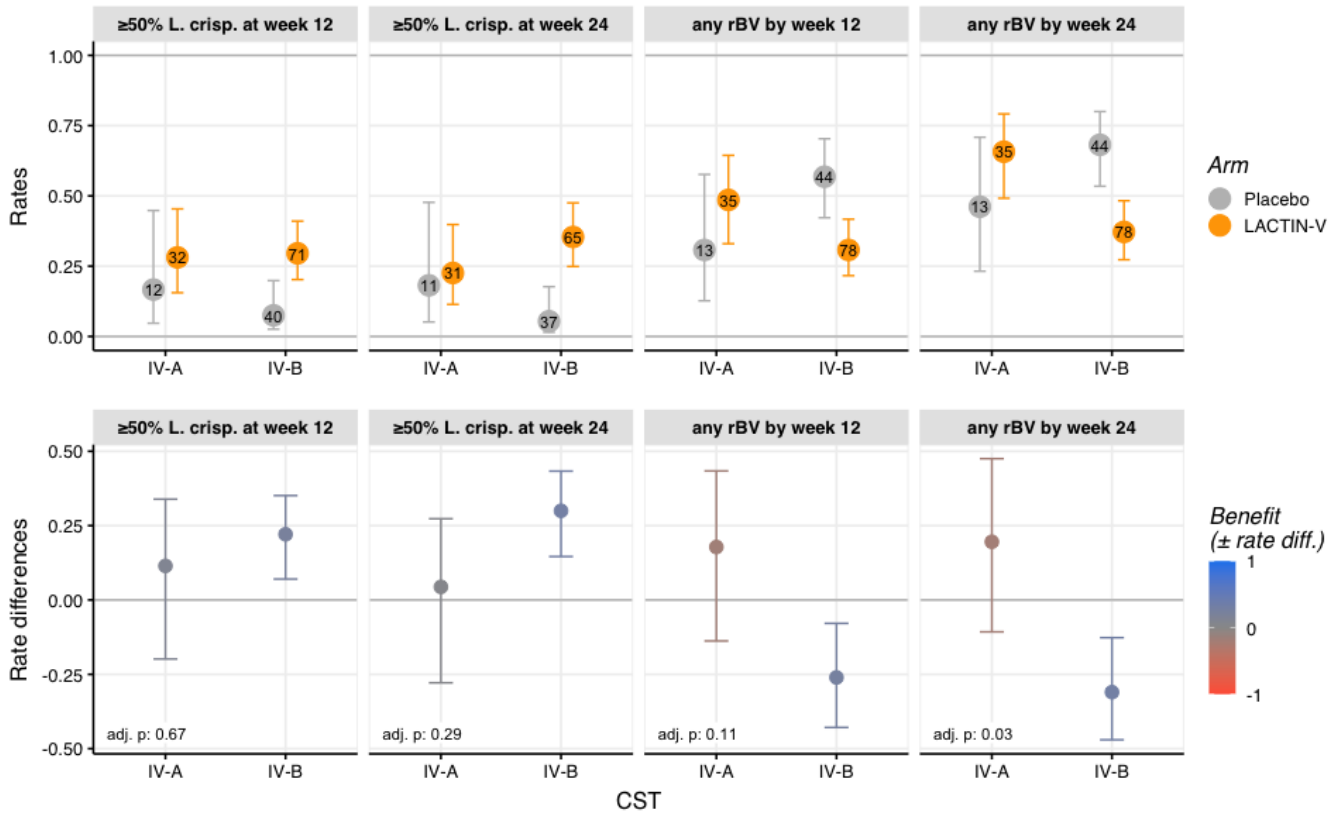


1395

1396 Rates and associated 95% CI of high-level *L. crispatus* colonization (≥50% of relative abundance) (y-
1397 axis) at week 12 or 24 (left two panels, top row) or rBV by Week 12 or 24 (right two panels, top row) by
1398 pre-MTZ CST in each arm (colors), and the corresponding rate differences and 95% CI between arms
1399 (bottom row), analyzed as in **Figure 5C-F**. Analysis is restricted to CSTs with at least two participants in
1400 each arm (*i.e.,* CSTs IV-A and IV-B). The color scale in the bottom row shows the degree of benefit
1401 (defined as the difference in rates between the two arms) in achieving *L. crispatus*-dominance (left
1402 panels) or reducing rBV (right panels), with blue indicating benefit with LBP treatment and red indicating
1403 benefit with placebo. *P*-values adjusted for multiple testing using the Benjamini-Hochberg correction of
1404 the analysis of deviance test for heterogeneity in treatment effects when stratifying participants by CST

1405 at the pre-MTZ visit. The centroid definition of CST IV-A includes *Ca*. Lachnocurva vaginae (BVAB1) as

1406 a predominant taxon while CST IV-B has higher abundance of *Gardnerella* and both share moderate

1407 *Prevotella* abundance[57].

1408 **Figure S6**

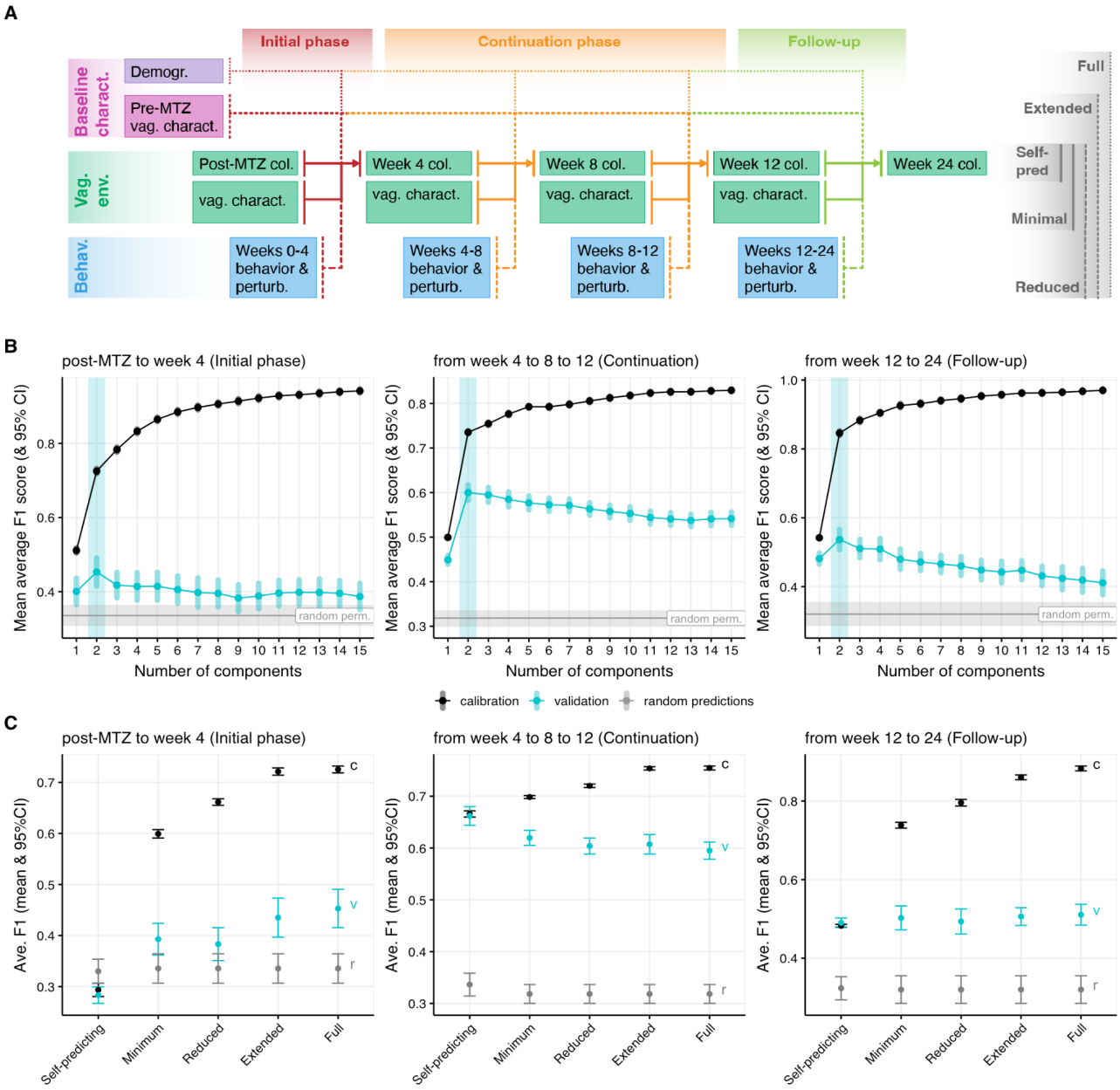


1409

1410 A. Diagram depicting MB-PLS-DA nested models. To assess whether blocks contributed to
1411 explaining colonization, we compared a series of nested models (far-right labels). The full model
1412 includes all blocks and variables, while the “self-predicting” model solely includes the microbiota
1413 categories at the previous visit.

B. Number of latent component selection by cross-validation for the initial phase (left), continuation phase (middle), and follow-up phase models (S6A). Mean (dots) and 95% CI (vertical segment) of the average F1 score (y-axis) obtained when including k latent components (x-axis) on 20 random calibration (black) or validation (turquoise) set. For reference, values obtained for random permutations of the response labels are shown by the horizontal gray line and band. The number of selected latent components is shown by the light turquoise vertical band (here k = 2 for all phases).

C. Contribution of nested models for the initial, continuation, and follow-up phase models. Mean and 95%CI of the average F1 score (y-axis) on the calibration (black, “c”), validation (turquoise, “v”), or for random predictions (gray, “r”) for each nested model (x-axis) including the number of latent components shown on the corresponding upper-panel.

1425 **Figure S7: Variables associated with microbiota categories in LACTIN-V recipients**

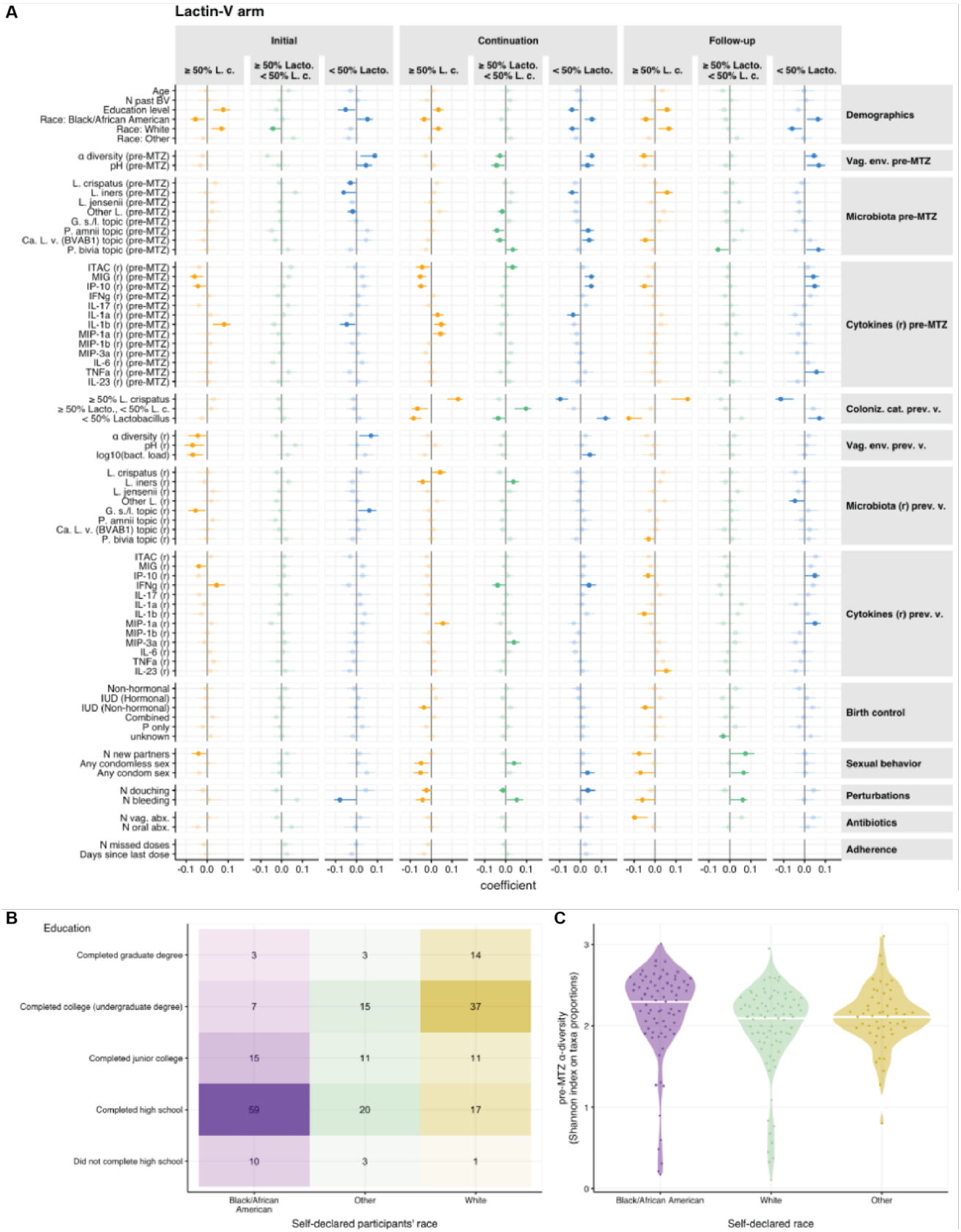
A
Lactin-V arm
Initial
Continuation
Follow-up
≥ 50% L. c.
≥ 50% Lacto. < 50% L. c.
< 50% Lacto.
Age
N past BV
Education level
Race: Black/African American
Race: White
Race: Other
Demographics
α diversity (pre-MTZ)
pH (pre-MTZ)
Vag. env. pre-MTZ
L. crispatus (pre-MTZ)
L. iners (pre-MTZ)
L. jensenii (pre-MTZ)
Other L. (pre-MTZ)
G. s./l. topic (pre-MTZ)
P. amnii topic (pre-MTZ)
Ca. L. v. (BVAB1) topic (pre-MTZ)
P. bivia topic (pre-MTZ)
Microbiota pre-MTZ
ITAC (r) (pre-MTZ)
MIG (r) (pre-MTZ)
IP-10 (r) (pre-MTZ)
IFNg (r) (pre-MTZ)
IL-17 (r) (pre-MTZ)
IL-1a (r) (pre-MTZ)
IL-1b (r) (pre-MTZ)
MIP-1a (r) (pre-MTZ)
MIP-1b (r) (pre-MTZ)
MIP-3a (r) (pre-MTZ)
IL-6 (r) (pre-MTZ)
TNFa (r) (pre-MTZ)
IL-23 (r) (pre-MTZ)
Cytokines (r) pre-MTZ
≥ 50% L. crispatus
≥ 50% Lacto., < 50% L. c.
< 50% Lactobacillus
Coloniz. cat. prev. v.
α diversity (r)
pH (r)
log10(bact. load)
Vag. env. prev. v.
L. crispatus (r)
L. iners (r)
L. jensenii (r)
Other L. (r)
G. s./l. topic (r)
P. amnii topic (r)
Ca. L. v. (BVAB1) topic (r)
P. bivia topic (r)
Microbiota (r) prev. v.
ITAC (r)
MIG (r)
IP-10 (r)
IFNg (r)
IL-17 (r)
IL-1a (r)
IL-1b (r)
MIP-1a (r)
MIP-1b (r)
MIP-3a (r)
IL-6 (r)
TNFa (r)
IL-23 (r)
Cytokines (r) prev. v.
Non-hormonal
IUD (Hormonal)
IUD (Non-hormonal)
Combined
P only
unknown
Birth control
N new partners
Any condomless sex
Any condom sex
Sexual behavior
N douching
N bleeding
Perturbations
N vag. abx.
N oral abx.
Antibiotics
N missed doses
Days since last dose
Adherence
-0.1 0.0 0.1
coefficient
B
Education
Completed graduate degree
Completed college (undergraduate degree)
Completed junior college
Completed high school
Did not complete high school
3 3 14
7 15 37
15 11 11
59 20 17
10 3 1
Black/African American
Other
White
Self-declared participants' race
C
pre-MTZ α-diversity (Shannon index on taxa proportions)
0
1
2
3
Black/African American
White
Other
Self-declared race

1426

1427 A. Coefficient of association (dots, x-axis) and associated bootstrapped 95% CI (horizontal
1428 segments) between explanatory variables (y-axis) and microbiota categories (colors, horizontal
1429 panels, see **Figure 6A**) for each phase of the trial (horizontal panels) for MB-PLS-DA models
1430 fitted on LBP recipient data (**Figure S6A**). Variables whose 95% CI include 0 are shown in
1431 transparent/lighter shades. Variables are shown grouped according to their assigned thematic
1432 blocks (**Figure 6A**, **Table S6**).
1433 B. Self-reported education levels are significantly associated with self-reported race ($\chi^2$ *p*-value <
1434 0.01)
1435 C. Pre-MTZ α-diversity is higher in Black or African American participants than in White participants
1436 (*p*-value of *t*-test on association coefficient < 0.05).

1437 **Figure S8: Multiblock analysis of factors associated with microbiota categories in placebo**
1438 **recipients**

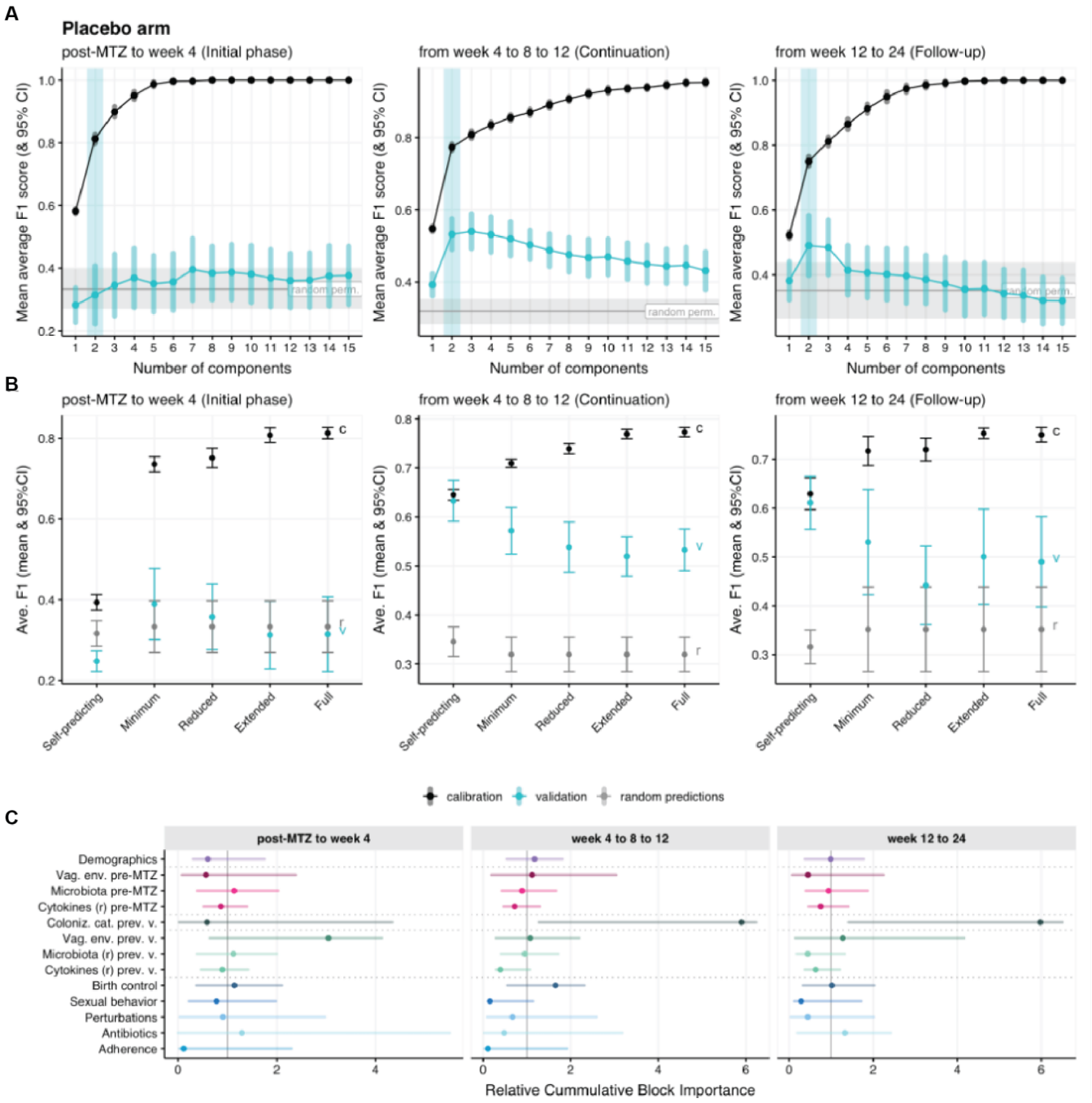


1439

1440 A. Number of latent component selection by cross-validation for the initial (left), continuation
1441 (middle), and follow-up phase (right) model fitted on the placebo arm data. Reads as **Figure S6B**.

1442 B. Contribution of nested models fitted on the placebo arm data for the initial (left), continuation
1443 (missing) and follow-up phase (right). Reads as **Figure S6C.**
1444 C. Relative cumulative importance indices in the placebo arm (x-axis, Methods) for each block (y-
1445 axis, color) for the initial phase model (post-MTZ to Week 4; left), continuation phase model (Week
1446 4 to 8 to 12; middle), and follow-up phase model (Week 12 to 24; right), analogous to portrayal of
1447 LBP arm in **Figure 6A**.

**Figure S9: Variables associated with microbiota categories in placebo recipients**

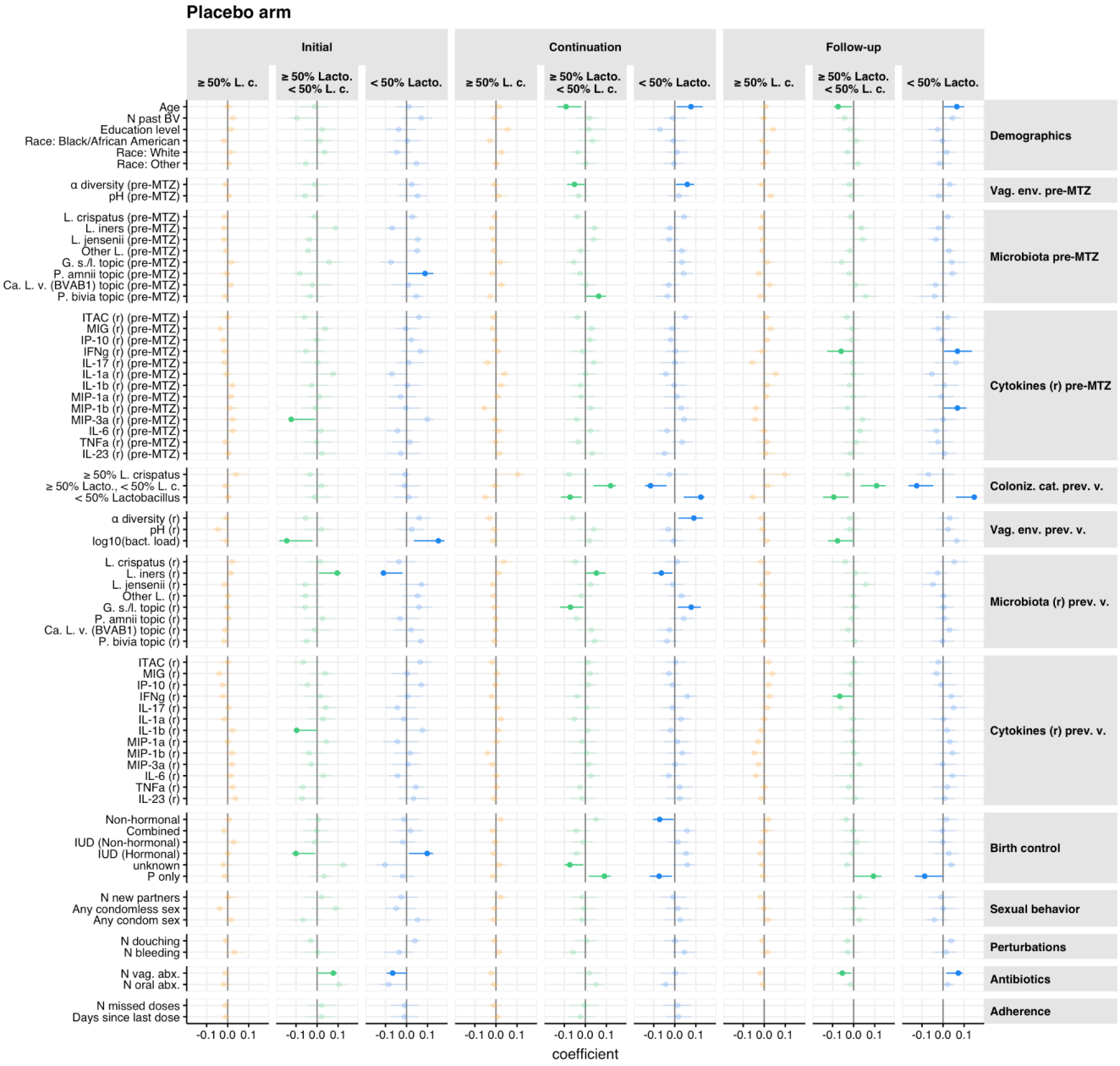


Coefficient of association (dots, x-axis) and associated bootstrapped 95% CI (horizontal segments) between explanatory variables (y-axis) and microbiota categories (colors, horizontal panels) for each phase of the trial (horizontal panels) when MB-PLS-DA models are fitted on the placebo arm participants' data. Variables whose 95% CI include 0 (suggesting no statistically significant associations) are shown

in transparent/lighter shades. Variables are shown grouped according to their assigned thematic blocks (**Figure 6A**, **S8C Table S6**).